ASD-TDR-62-1075

Influence of Residual Stresses on Random Fatigue Life, in Bending, of Notched 7075 Aluminum Specimens

TECHNICAL DOCUMENTARY REPORT NO. ASD-TDR-62-1075

December 1962

Directorate of Materials and Processes
Aeronautical Systems Division
Air Force Systems Command
Wright-Patterson Air Force Base, Ohio

Project No. 7351, Task No. 735106

(Prepared under Contract No. AF 33(616)-7042 by Columbia University, New York, New York; R. A. Heller, M. Seki, A. M. Freudenthal, authors)

NOTICES

When Government drawings, specifications, or other data are used for any purpose other than in connection with a definitely related Government procurement operation, the United States Government thereby incurs no responsibility nor any obligation whatsoever; and the fact that the Government may have formulated, furnished, or in any way supplied the said drawings, specifications, or other data, is not to be regarded by implication or otherwise as in any manner licensing the holder or any other person or corporation, or conveying any rights or permission to manufacture, use, or sell any patented invention that may in any way be related thereto.

Qualified requesters may obtain copies of this report from the Armed Services Technical Information Agency, (ASTIA), Arlington Hall Station, Arlington 12, Virginia.

This report has been released to the Office of Technical Services, U.S. Department of Commerce, Washington 25, D.C., for sale to the general public.

Copies of this report should not be returned to the Aeronautical Systems Division unless return is required by security considerations, contractual obligations, or notice on a specific document.

Influence of Residual Stresses on Random Fatigue Life, in Bending, of Notched 7075 Aluminum Specimens

TECHNICAL DOCUMENTARY REPORT NO. ASD-TDR-62-1075

December 1962

Directorate of Materials and Processes
Aeronautical Systems Division
Air Force Systems Command
Wright-Patterson Air Force Base, Ohio

Project No. 7351, Task No. 735106

(Prepared under Contract No. AF 33(616)-7042
by Columbia University, New York, New York;
R. A. Heller, M. Seki, A. M. Freudenthal,
authors)

Foreword

This report was prepared by the Department of Civil Engineering and Engineering Mechanics of Columbia University under USAF Contract No. AF 33(616)-7042. The contract was initiated under Project No. 7351, "Metallic Materials," Task No. 735106, "Behavior of Metals." The work was administered under the direction of the Directorate of Materials and Processes, Deputy for Technology, Aeronautical Systems Division, with Mr. D. M. Forney, Jr., acting as project engineer.

This report covers the period of work, August 1, 1960 to August 31, 1962.

The cooperation and continued interest of Mr. D. M. Forney, Jr., is gratefully acknowledged.

Abstract

Theoretical and experimental results of investigations conducted to determine the effects of residual stresses on fatigue damage accumulation and fatigue life under both constant amplitude and randomized exponential stress distributions, of 7075-T6 circumferentially notched rotating bending specimens are presented. The variation of the strength reduction factor as a function of prestress and load spectrum is examined. An approximate analysis of the elastic-plastic stress distribution at the minimum cross section is suggested on the basis of which fatigue behavior can be predicted. The results indicate that the linear (Miner) cumulative damage rule quite generally overestimates fatigue lives except in the alternating plasticity range and that the endurance limit is considerably reduced as a result of stress interaction, provided that in the application of the linear damage rule the S-N-diagram for the prestressed specimen is used. In the range of alternating plasticity at the root of the notch $10^3 < N < 10^4$ the linear rule consistently underestimates the fatigue life.

This technical documentary report has been reviewed and is approved.

W. J. TRAPP
Chief, Strength and Dynamics Branch
Metals and Ceramics Laboratory
Directorate of Materials and Processes

Table of Contents

List of Illustrations

List of Illustrations (Cont'd.)

List of Tables

List of Symbols

A	constant of $S - V_s$ relation
a	radius of minimum cross section
B, B'	constants of Neuber's equations
C, C'	" " "
D, D'	" " "
E'	" " "
e	base of natural logarithms
h	parameter of exponential load distribution
i	i^{th} stress level
J_2'	second invariant of stress deviator
K_f	strength reduction factor under constant amplitude load
K_{fR}	strength reduction factor under randomized loads
K_t	theoretical elastic stress concentration factor
k, k_o	parameters in Neuber's equations
L, L_∞	probability of survival, probability of infinite life
M	bending moment
m	stress reduction ratio
N	fatigue life in general
N_s, N_R'	fatigue life under constant and variable amplitude stress
N_o	minimum fatigue life at $L = 1$
P	direct load
$p(s^*)$	probability density function for stresses
p_i	frequency of occurrence of i^{th} stress level
r	radial coordinate
S, S_i	nominal bending stress amplitude for notched specimens
S^*, S_i^*	nominal bending stress amplitude for smooth specimens

List of Symbols (Cont'd.)

S_e	constant amplitude endurance limit
S'_e	reduced endurance limit due to stress interaction
S_p	nominal prestress
S_r, S_θ, S_z	radial, tangential, and longitudinal components of stress
S_1, S_m	lowest and highest stress level in spectrum
S_y	yield strength of smooth specimens
s, s_i, s^*, s^*_i, s_e, s'_e, s_p, s_1, s_m	stress ratios; nominal stress divided by ultimate tensile strength, σ_u, of smooth specimens
V	characteristic fatigue life in general, at probability level $L = 1/e$
V_m	characteristic constant amplitude fatigue life at maximum stress level in spectrum
V_R, V'_R	linear estimate and observed fatigue life at probability level $L = 1/e$
V_{si}, V'_{si}	real and fictitious constant amplitude fatigue life at i^{th} stress level and $L = 1/e$
z	longitudinal coordinate
$\alpha, \alpha_s, \alpha_R$	constants of probability of survival function in general, for constant, and for variable stress amplitude
Δs^*, Δs	stress ratio difference for smooth and notched specimens
ν	constant of $S - V_s$ relation
$\bar{\nu}$	Poisson's ratio
π	= 3.14159
ρ	radius of curvature at root of notch
σ_u	ultimate tensile strength of smooth specimens

List of Symbols (Cont'd.)

θ	tangential coordinate
τ_o	octahedral shear stress
τ_{oa}, τ_{om}	alternating and mean octahedral shear stress
$\bar{\omega}$	average stress interaction factor; reciprocal of cumulative cycle ratio

1. Introduction

An extensive study of fatigue damage accumulation under variable-amplitude load cycles derived from exponential distributions of load amplitudes of different severity has conclusively shown[1] that, for unnotched small metal specimens in rotating bending, fatigue damage accumulation at low and medium stress amplitudes is considerably accelerated by a very small number of interspersed high stress-amplitudes, so that the application of the widely used linear damage accumulation rule leads to an overestimate of the variable-amplitude fatigue life of the specimen. The relevance of these conclusions for the design of structural parts and connections of airframes and other structures has been questioned on the basis of the facts that (a) the specimens are small and loaded in rotating bending; (b) neither notch effects nor the effect of residual stresses, both characteristic of the conditions of use of the material in a structure have been considered.

Both objections are obviously valid, but the problem of extrapolations of fatigue test results obtained under conditions (a) to fatigue behavior of structural members and connections is one that is still waiting for an adequate solution considering the fact that only small-specimen tests can be performed with sufficient replication to yield statistically significant results. On the other hand, the effect of notches and residual stress can be studied on small specimens and their fatigue behavior compared to that of unnotched specimens free of residual stresses. While there is no assurance

---

Manuscript released by the authors November 1962 for publication as an ASD Technical Documentary Report.

that the quantitative differences found in such comparisons are in any way representative of the differences arising in full scale structures, it is not unreasonable to assume that the trend of the results in small-scale specimens will be similar to that expected in large structural parts.

An investigation has therefore been undertaken to evaluate the effect of notches as well as the effect of residual stresses, produced in the notched section by axial (compressive or tensile) prestrain, on the fatigue life of specimens subjected to a randomized sequence of rotating bending stress amplitudes arising from an exponential distribution. In particular, it seemed desirable to study the relation between an induced compressive residual stress and the severity of the test-spectrum in its effect on the random fatigue life in order to test the hypothesis that only a prestress in excess of or at least equal to the highest stress amplitude of the applied spectrum will have a stable effect on the fatigue life while a prestress of the order of magnitude of the mean or median amplitude of the spectrum may have only a transient effect, if any. The importance of the study of this effect derives from the increasing application of compressive residual stresses as a procedure of reducing the fatigue sensitivity of structural parts or increasing their fatigue life.

2. Notch Geometry and Elastic Stress Distribution

The investigation was carried out on 7075-T6 aluminum alloy, with material properties shown in Table 1, and conducted on specially built random fatigue machines. Because of the capacity of the testing equipment and the requirement of accurate machining the following notch geometry was adopted: 3/8 inch diameter extruded rods were machined to

5/16 inch with a 30° "V" notch having a root radius, $\rho = 0.01$ in. and a minimum diameter, $2a = 3/16$ in. as shown in Fig. 1. The notches were turned on a high speed lathe and were not polished.

The theoretical elastic stress distribution at the smallest cross section was determined using expressions developed by Neuber[2] for a deep hyperbolic notch (Fig. 2), which give reasonable approximations for the chosen geometry.

The general equations have been simplified to yield the distribution of the three principal stress components at the smallest cross section of the specimen for both direct stress and bending.

It is to be noted that the general equation for the tangential component as given by Neuber for the case of simple tension is in error. Equation V.50., in his book, from which the tangential stress concentration factor, Eq. V.60., is to be derived, will not yield that result and is dimensionally incorrect. Because the derivation of the correct expression, for the most general case, is a prodigious task, improved and simplified terms were derived only for the stress components at the smallest cross section.

For tension or compression with a nominal direct stress $S_p = \frac{P}{\pi a^2}$, where P is the applied force and a the minimum radius

$$S_z = \frac{1}{k}\left[B + 2C(\bar{\nu} - 1)\right] + \frac{1}{k^3}(B - A) \qquad (2\text{-}1)$$

$$S_r = -\frac{1}{k}\left[\frac{A}{1 + k} + 2C\,\bar{\nu}\right] - \frac{1}{k^3}(B - A) \qquad (2\text{-}2)$$

$$S_\theta = \frac{1}{k}\left[\frac{A}{1+k} - B - 2C\,\bar{\nu}\right] \tag{2-3}$$

with the constants

$$C = -\frac{S_p}{2}\,\frac{1+k_o}{1+2\bar{\nu}k_o+k_o^2} \tag{2-4}$$

$$A = (1-2\bar{\nu})(1+k_o)C \tag{2-5}$$

$$B = A - Ck_o^2 \tag{2-6}$$

where S_z, S_r and S_θ are the longitudinal, radial and tangential components of stress at the smallest cross section, $\bar{\nu}$ is Poisson's ratio, $k_o = 1/\sqrt{a/\rho+1}$, $k = \sqrt{1-(r^2/a^2)(1-k_o^2)}$, ρ the radius of curvature at the root of the notch, and r the radial coordinate.

For bending with a nominal bending stress $S = \frac{4M}{\pi a^3}$ where M is the bending moment

$$S_z = \frac{\sqrt{1-k^2}}{k}\left[-2C' + (3-2\bar{\nu})D' + \frac{1}{k^2}\left(A' + \frac{2}{3}B' + D'\right)\right] \tag{2-7}$$

$$S_r = \frac{\sqrt{1-k^2}}{k}\left[\frac{A'}{(1+k)^2} + \frac{2}{3}B' - 2C' + 2D'\bar{\nu} - \frac{1}{k^2}\left(A' + \frac{2}{3}B' + D'\right)\right] \tag{2-8}$$

$$S_\theta = \frac{\sqrt{1-k^2}}{k}\left[\frac{-A'}{(1+k)^2} - \frac{2}{3}B' - 4C'\bar{\nu} + (2\bar{\nu}-1)D'\right] \tag{2-9}$$

with constants

$$A' = -\frac{4D'}{E'}(-1 + 3\bar{\nu} - 2\bar{\nu}^2)(1 + k_o)^2 \qquad (2\text{-}10)$$

$$B' = (C' + D')(1 - 2\bar{\nu}) \qquad (2\text{-}11)$$

$$C' = \frac{2D'}{E'}[-3(1-\bar{\nu}) + (-1+2\bar{\nu})k_o + (1+\bar{\nu})k_o^2] \qquad (2\text{-}12)$$

$$E' = 4k_o[(-1 + 2\bar{\nu}) + (1 + \bar{\nu})k_o] \qquad (2\text{-}13)$$

$$\frac{D'}{E'} = \frac{3M}{8\pi(1-k_o)^2(1-\bar{\nu})[3+k_o(1+\bar{\nu})(4+k_o^2)+(1+4\bar{\nu})k_o^2]} \qquad (2\text{-}14)$$

Equations (2-1) to (2-14) were evaluated numerically for the particular geometry used and the three components of stress were plotted in Figs. 3 and 4 for direct stress and bending respectively. In addition to the principal stresses the second invariant of the stress deviator

$$J_2' = \frac{1}{6}\left[(S_z - S_\theta)^2 + (S_\theta - S_r)^2 + (S_r - S_z)^2\right] \qquad (2\text{-}15)$$

and the octahedral shear stress

$$\tau_o = \sqrt{\frac{2}{3} J_2'} \qquad (2\text{-}16)$$

were calculated and τ_o was also plotted on Figs. 3 and 4. The elastic stress concentration factors K_t based on the peak principle stress can be obtained from Figs. 3 and 4 for direct stress: $K_t = 3.23$; for bending: $K_t = 2.55$. While the stress concentration factors based on the octahedral shear stress are for direct stress: $K_t = 1.34$; for bending: $K_t = 1.06$.

3. Residual Stress Distribution

When a notched specimen is strained so as to yield at the root of the notch a self-equilibrating residual stress field is established on unloading. A rigorous analytical solution of the elastic-plastic stress distribution in a triaxial state of stress has so far not been found, but various approximate solutions have been proposed in the literature. Thus Neuber[3] has developed a method for the calculation of post yield stresses based on a nonlinear stress-strain law. A complete solution is, however, available only for a state of pure shear. In a recent publication[4], the same procedures are applied for tension in a biaxial state of stress such as a flat notched specimen.

Uzhik[5] has shown that an approximate solution for the distribution of the largest principal stress in a notched specimen can be obtained based on either the St. Venant or the Von Mises yield condition. According to that approximation the largest principal stress at the boundary of the elastic and elastic-plastic zones should have a value

$$S_{z_p} = \frac{S_z S_y}{S_z - S_r}$$

where S_z and S_r are the values of the elastic stresses at the boundary when plastic deformation is initiated at the root of the notch. The determination of the boundary as well as the distribution of stresses is, however, not clearly explained.

A number of experimental investigations[6,7,8] have been conducted on flat notched specimens in which the measurements of stresses and strains are comparatively easy, but no experimental measurements of residual stresses in circumferentially notched bars are presently available.

A combination of analytical and graphical methods will be used in this investigation in the following manner.

Yielding will be expressed in terms of the octahedral shear stress. According to the Mises condition,

$$J_2' = \frac{1}{3} S_y^2 \quad \text{or} \quad \tau_o^2 = \frac{2}{9} S_y^2 \quad \text{since} \quad \tau_o = \sqrt{\frac{2}{3} J_2'} \qquad (3\text{-}1)$$

where S_y is the yield strength of the plane material in simple tension. For 7075 aluminum this is 92.5 per cent of the ultimate tensile strength, σ_u = 82,000 psi[9]. Consequently, when $\tau_o = .436\sigma_u$, yielding must be expected to occur.

The use of Eq. (3-1) implies that the material is not work hardening, an assumption that does not seem unreasonable because of the high yield strength of the material.

Derived from Neuber's[3] elastic stress distributions the octahedral shear stress, τ_o, is plotted in Fig. 5a. Where the yield condition, Eq. (3-1), is satisfied the stress intensity cannot increase further; however, to satisfy conditions of equilibrium, the stress in the elastic portions of the cross section must increase and the area added to the stress distribution curve should therefore be equal to that eliminated above the yield condition. If the elastic-plastic section is then unloaded by subtracting the elastic stress distribution associated with the same force, from the elastic-plastic one, the obtained residual stress pattern will be a reasonable approximation to the real residual stress field.

Should yielding occur on unloading a second area readjustment becomes necessary to obtain the residual stress distribution.

Two basic assumptions are made in the above analysis: First, octahedral shear stresses at a point can be numerically superimposed; that is, their directions are assumed not to change during loading and unloading. Second, that the shape of the elastic portion of the elastic-plastic distribution remains similar to the original elastic one.

To permit a simple discussion of the results in terms of stress it will be assumed that the initial loading will produce positive and unloading a negative octahedral shear stress.

4. Alternating Bending Superimposed on Residual Stress

Once the residual stress distribution has been determined for a particular pre-strain level, the superposition of a bending cycle can easily be accomplished in a manner similar to that described above.

If the pre-strain was tensile resulting in a compressive residual stress field ("negative" octahedral shear stress) the compressive half of the alternating bending cycle will be considered first. If the elastic octahedral shear stress of the bending cycle shown in Fig. 4 is substracted from the octahedral residual stress, it will invariably cause yielding. Hence the elastic-plastic correction must be applied again as described in Sec. 3. Subsequently, the bending stress is removed and finally reversed with the addition of twice the elastic octahedral bending stress distribution, correcting again for yielding and plastic deformation. The process may

have to be repeated until a steady-state condition is achieved. For a compressive pre-strain, the process is simply inverted.

Figures 5b and 6 show the final bending stress distributions for various pre-strain and alternating bending stress levels.

The initial stress distribution will not remain unchanged once a crack has formed at the root of the notch; stress redistribution has been observed by a number of investigators on flat specimens[5,8] but the examination of initial conditions will allow a general determination of behavior under cyclic loading.

The following conclusion can be based on the above analysis: No residual stress will result from a pre-stress ratio $s_p < \pm .32$, stress-ratio being defined as the nominal stress, S_p, divided by the ultimate tensile strength, σ_u, of the smooth material, while $s_p > \pm .65$ will produce yielding both on loading and unloading as shown in Figs. 5 and 6.

If the pre-stress ratio $s_p > \pm .50$ a superimposed alternating stress of $s_p < .21$ will produce no stress reversal and consequently pulsating tension or pulsating compression fatigue will take place depending on the sign of the residual stress at the root of the notch. If this stress is positive, that is tensile, long fatigue lives will be achieved only for very low levels of alternating stress, while if it is negative or compressive no fatigue will result and lives will be infinitely long (Fig. 6c).

For bending stress ratios $.21 < s < .41$ various amounts of stress reversal, with non-zero mean stress, will be observed at the root (6a, b, d).

When s is increased above .41 yielding will take place both in tension and compression in every cycle and stresses at the base of the notch will alternate with zero mean (Fig. 5b, 6e, f, g); fatigue is replaced by alternating plasticity.

With a tensile residual stress field fatigue lives will be shortened as soon as stress reversal takes place while for alternating plasticity, lives will be extremely short.

Bending superimposed on a compressive residual stress will produce an interesting effect. For low and intermediate bending stresses, though stress reversal will cause tension at the root of the notch, a predominantly compressive field will be maintained immediately below the surface as is evident from an examination of Figs. 6a, d and f. Crack propagation will be arrested by this compression and long fatigue lives can be expected. With increasing bending stresses the compressive stress field diminishes and fatigue is replaced by alternating plasticity with short lives. The amount of bending that will still produce subsurface compression depends on the depth of the residual stress field, which in turn is a function of the applied pre-stress. Similar stress patterns were observed experimentally by others on flat notched specimens, though the compressive stress field was not apparent probably because of low pre-stress levels.[10]

The fatigue behavior of pre-stressed circumferentially notched specimens in bending is summarized in Table 2.

5. Constant Amplitude Fatigue Tests

7075 Aluminum specimens were prepared with circumferential notches as shown in Fig. 1. They were pre-stressed in compression or tension to various pre-stress levels, S_p ,

varying between $-1\sigma_u$ and $+1.45\sigma_u$ to induce tensile and compressive residual stresses respectively. Rotating bending fatigue tests were subsequently performed on these specimens using "Krouse" constant amplitude machines for the determination of complete S-N-L relationships at various values of S_p .

Ten specimens were tested at each combination of bending stress and pre-stress level, providing a total of about 300 constant amplitude results. At the highest bending stress levels only three tests were performed in each case because of the very narrow spread of short fatigue lives. The results shown in Table 3 were statistically analyzed using the three-parametric distribution of extreme values,[11] and were plotted on extreme value probability paper in Figs. 7a and 7b.

The three parameters: N_o , the minimum life, V the characteristic life at the probability level $L = 1/e$, and the slope α of the probability function

$$L = \exp\left[-\frac{N - N_o}{V - N_o}\right]^{\alpha} \qquad (5\text{-}1)$$

for the case of constant amplitude stress designated as N_o, V_s and α_s are also given in Table 3.

The characteristic values were plotted as conventional $S\text{-}V_s$ diagrams in Fig. 8 which in addition contains a similar curve for smooth specimens for purposes of comparison.[9]

The equations of the $S\text{-}V_s$ relations may be expressed as

$$V_s = A(s - s_e)^{-\nu} \qquad (5\text{-}2)$$

where A and ν are constants, s is the bending stress amplitude ratio, and s_e the conventional endurance limit ratio. The values of the constants for all curves are presented in Table 4.

An examination of Fig. 8 will show that the conclusions reached in Sec. 4 and summarized in Table 2 are valid.

Table 2 suggests also that, at the root of the notch, the effects of a residual stress field are similar to those of an applied mean stress. A modified Goodman diagram can therefore be drawn to indicate possible combinations of mean and alternating stress to produce constant values of life. Such diagrams have been constructed for $V_s = 10^8$, 10^5 and 10^4 cycles and are presented in Fig. 9. Similar curves were obtained by Sigwart[12] for direct stress fatigue.

The central sloping portions of each curve indicate that the material is elastic, while when one of the horizontal limits is reached yielding takes place. Two values of alternating stress may be associated with each value of compressive mean stress: one for the elastic range and another for the case of pulsating and alternating plasticity. The increase in fatigue strength with compressive residual stress is quite apparent.

The beneficial or detrimental effects of residual stress may best be illustrated by plotting the ratio of fatigue lives of pre-stressed and not-pre-stressed specimens versus the pre-stress level for various constant amplitude bending stress levels as shown in Fig. 10. While the increase in life as a result of compressive residual stresses is quite significant, the reduction due to tensile residual stress is not very prominent. The variation of the endurance limit as a function of prestress is shown in Fig. 11.

The Strength Reduction Factor

The fatigue strength of specimens and structural components having high stress concentrations is, in general, considerably lower than that of smooth specimens. The strength reduction factor, K_f , defined as the strength ratio of smooth and notched specimens at the same constant amplitude fatigue life, is usually greater than unity. With a superimposed residual stress field the apparent strength reduction factor may, however, have a value less than one signifying an increase in strength rather than a reduction.

The strength reduction factor has been plotted in Fig. 12. The diagram shows that K_f first increases with increasing fatigue life, then decreases. The most significant peaks, occurring in tests with tensile residual stress, indicate the most dangerous regions in fatigue life and strength. At short fatigue lives corresponding to high stress levels, alternating plasticity takes place and K_f is low; as lives increase, true alternating stress fatigue occurs which for specimens with tensile residual stress (s_p = -.75, -1) coincides with the existence of a subsurface tensile crack opener and here K_f becomes very large. When compressive residual stresses are present (s_p = .75, 1, 1.34) the crack opener is replaced by a compressive crack stopper and K_f decreases. For low stress levels alternating stress fatigue is replaced by pulsating fatigue at largely elastic conditions and K_f reduces further.

It is somewhat more difficult to explain a peak in the K_f curve for non-prestressed specimens. At high stresses alternating plasticity and at intermediate levels true fatigue takes place in these specimens also and K_f increases.

The subsequent decrease at long lives or low alternating stresses can be again attributed to a condition of pulsating stress which is induced at the root of a crack in spite of the fact that the nominal stress is completely reversed. This phenomenon has been observed by Isibasi[13] and by Harris[14] in steels and is attributed to residual stresses resulting from the sharp stress concentration at the tip of a crack.

6. Cumulative Damage Under Randomized Exponential Stress Distributions

It has been shown in earlier publications[1,15] that the effects of stress interaction in variable amplitude fatigue tests on smooth specimens are mostly damaging and result in a reduced endurance limit.[16] Observed fatigue lives are considerably shorter than estimated[17] on the basis of the linear damage rule.[18]

Experiments performed by Hardrath and associates[19] on notched specimens of 7075-T6 aluminum with continuously variable stress amplitudes and sinusoidal, exponential, and gust frequency modulations indicate that, in the great majority of cases, the linear damage rule overestimates fatigue lives. The present investigation shows that under randomized exponential stress distributions cumulative damage is intensified, cumulative cycle ratios are less than one, and the endurance limit is lowered even when residual stresses are present. Cumulative cycle ratios greater than one were observed only in low cycle tests with tensile residual stresses where fatigue is replaced by alternating plasticity.

Strength Reduction Factor

The random fatigue strength reduction factor, K_{fR}, de-

fined as the constant by which all stress levels of a spectrum must be divided to produce the same fatigue life in a notched specimen as that of a smooth specimen under a proportional stress distribution, was determined experimentally using several exponential stress spectra. The randomized exponential stress distribution, whose frequency function is $p(s^*) = he^{-h(s^* - s_1^*)}$ from which the proportion of cycles at the i^{th} stress level,

$$p_i = \int_{s_i^*}^{s_{i+1}^*} p(s^*)ds^* = e^{-ih\Delta s^*}(e^{h\Delta s^*} - 1) \qquad (6\text{-}1)$$

can be computed, has been used to determine its effects on the fatigue life of smooth specimens.[15] In the above expression h is the only parameter of the distribution and $\Delta s^* = s_{i+1}^* - s_i^* = .1$, where starred quantities refer to smooth specimens, is constant. The frequencies of occurrence, p_i, used in the tests are listed in Table 5, and the characteristic values of fatigue lives in Tables 6 and 7 under smooth specimens.

The frequencies of occurrence, p_i, of Table 5 were also used, to determine fatigue lives of notched specimens under proportionally reduced stress distributions for which the stress levels $s_i = s_i^*/m$ and $\Delta s = \Delta s^*/m$. Various values of m were chosen until the fatigue life of notched specimens and smooth specimens was nearly identical. The interpolated value of m was then designated as the random strength reduction factor K_{fR}.

Specially built rotating bending fatigue machines[20] were used in the investigation. The machines are able to apply

up to 7 electro-magnetically adjustable stress levels in any tape programmed sequence in blocks of 12 cycles to a specimen rotating at a speed of 3600 RPM. The program consists of 1000 load impulses of 12 cycles each after which it is repeated.

Ten specimens were tested at each combination of three slope parameters h, three s_1^*, and several m values; a total of over 600 random tests were performed. The results were statistically analyzed and the relevant parameters N_o, V_R' and α_R were computed using again the three parametric distribution of extreme values [Eq. (5-1)]. The characteristic values of fatigue lives, V_R', are listed in Tables 6 and 7 with zero prestress, while all test results and parameters are presented in Table 8 and are plotted on extremal probability paper on Fig. 13.

A series of tests were also performed on specimens previously subjected to prestress to investigate the effects of residual stress on the strength reduction factor under random loading. The experimental determination of the random strength reduction factor was carried out in the manner described above. These results are also presented in Tables 7 and 8 and in Fig. 13.

The strength reduction factor K_{fR} has been plotted as a function of prestress for three different values of the load parameter in Fig. 14.

It is apparent from a comparison of Figs. 12 and 14 that the variation of h has little effect on K_{fR} and a reasonable estimate may be obtained for this parameter by assuming it to be equal in value to that of K_f for an equivalent life at constant stress amplitude.

The effects of residual stresses on random fatigue life

are shown in Fig. 15 where curves are presented for two constant values of the ratio m. The increase in life with compressive residual stress (positive prestress) is much greater than the reduction due to tensile residual stress.

A plot of the experimentally obtained fatigue lives V'_R versus the linear estimate V_R for this life is shown in Fig. 16; it becomes quickly apparent that in the majority of cases the linear rule overestimates fatigue lives by factors as large as 100. It is, however, possible to obtain more conservative estimates using a fictitious $S - V'_s$ relationship in conjunction with a quasilinear damage rule[1] of the form

$$\frac{1}{\sum p_i / V'_{si}} \tag{6-2}$$

and

$$V'_{si} = V_m \left(\frac{s_m - s'_e}{s_i - s'_e} \right)^{\nu} \tag{6-3}$$

where V'_{si} is the fictitious constant amplitude fatigue life at the i^{th} stress level, V_m the constant amplitude life at the maximum stress ratio, s_m, of the spectrum computed from Eq. (5-2), ν the constant of Eq. (5-2) and s'_e is the reduced endurance limit ratio and the only unknown parameter of the solution. The computed values of s'_e are listed in Tables 6 and 7. Though the dependence of this parameter on the load spectrum is established beyond a doubt, the exact relationship governing stress interaction phenomena is not yet known.

References

1. Freudenthal, A. M. and Heller, R. A., "On Stress Interaction in Fatigue and a Cumulative Damage Rule," J. Inst. Aero/Space Sci., V. 26, No. 7, (1959), p. 431.

2. Neuber, H., "Kerbspannungslehre," Second Ed., Springer, Berlin (1958), p. 97, 104.

3. Ibid., p. 186.

4. Neuber, H., "Research on the Distribution of Tension in Notched Construction Parts," WADD TR-60-906 (1961).

5. Uzhik, G. V., "A Contribution to the Theory of Fatigue of Metals," IUTAM Colloq. on Fatigue, Springer, Berlin (1956), p. 278.

6. Forrest, P. G., "Influence of Plastic Deformation on Notch Sensitivity in Fatigue," Int. Conference on Fatigue of Metals, ASME, London. Session 2, Paper 11 (1956).

7. Blotherwick, A. B. and Olson, B. K., "Stress Redistribution in Notched Specimens Under Cyclic Stress," ASD TR 61-451 (1961).

8. Taira, S. and Murakami Y., "Residual Stresses Produced by Plastic Tension in Notched Plate Specimens and Fatigue Strength," Bull. Japan Soc. Mech. Engr., V. 4, No. 15, (1961), p. 453.

9. Freudenthal, A. M., Heller, R. A., and O'Leary, P. J., "Cumulative Fatigue Damage of Aircraft Structural Materials," Pt. I and II, WADC TN 55-273 (1955-56).

10. Rosenthal, D., Sines, G. and Zizicas, G., "Effect of Residual Compression on Fatigue," Welding Res. Suppl. March (1949), p. 98 s.

11. Freudenthal, A. M. and Gumbel, E. J., "Physical and Statistical Aspects of Fatigue," Adv. Appl. Mech., V. 4 (1956), p. 117.

12. Sigwart, H., "Influence of Residual Stresses on the Fatigue Limit," Int. Conference on Fatigue of Metals ASME, London, Session 3, Paper 6 (1956).

13. Isibasi, T., "On the Branch Point of Notched Fatigue Specimens," Proc. 6th Japanese Nat. Congress for Appl. Mech. (1956).

14. Harris, W. J., "Metallic Fatigue," Pergamon, London (1961), p. 21.

15. Freudenthal, A. M. and Heller, R. A., "On Stress Interaction in Fatigue and a Cumulative Damage Rule," WADC TR 58-69 (1961).

16. Heller, R. A., "The Endurance Limit in Randomized Variable Fatigue Tests," Materials Research, V. I, No. 1 (1962), p. 55.

17. May, A. N., "Fatigue Under Random Loads," Nature, V. 192, No. 4798 (1961), p. 158.

18. Miner, M. A., "Cumulative Damage in Fatigue," J. Appl. Mech., V. 12 (1945), p. A-159.

19. Hardrath, H. F., Utley, E. C. and Guthrie, D. E., "Rotating Beam Fatigue Tests of Notched and Unnotched 7075 T-6 Aluminum Alloy Specimens Under Stresses of Constant and Variable Amplitudes," NASA, TN-D-210 (1959).

20. Freudenthal, A. M., "A Random Fatigue Testing Procedure and Machine," Proc. Am. Soc. Test. Mats., V. 53 (1953), p. 896.

Table 1

Physical Properties of 7075 T6 Aluminum

Ultimate Tensile Strength σ_u ksi	Yield Strength in Tension S_y ksi	Modulus of Elasticity EX10^{-6} ksi	Poisson's Ratio $\bar{\nu}$
82	76	10	.333

Table 2

General Bending Fatigue Behavior of Circumferentially Notched Specimens with Superimposed Residual Stress

Bending Stress ratio	Tensile Residual Stress	No Residual Stress	Compressive Residual Stress
Low Level $.1 < s < .21$	Pulsating tension fatigue $10^5 < N < \infty$	Reversed stress with pulsating fatigue $10^6 < N < \infty$	Pulsating compression, no fatigue $N = \infty$
Intermediate level $.21 < s < .50$	Alternating stress fatigue with subsurface crack opener $10^4 < N < 10^5$	Reversed stress fatigue $10^4 < N < 10^6$	Alternating stress fatigue with subsurface crack stopper $10^7 < N < \infty$
High level $.50 < s < .75$	Alternating plasticity $10^3 < N < 10^4$	Alternating plasticity $10^3 < N < 10^4$	Alternating plasticity $10^3 < N < 10^4$

Table 3

Number of Cycles to Failure, N_s , in Thousands, Under Constant Amplitude Stress

Prestress Ratio s_p	Stress Amplitude S_i ksi	55	34	10	7
	Specimen No.				
	1	1.0	7.0	214.0	925.0
	2	1.1	7.0	216.0	1386.0
	3	1.2	7.0	217.0	1525.0
	4		7.0	224.0	1530.0
	5		8.0	232.0	1571.0
	6		8.0	250.0	--
-1.00	7		8.0	286.0	--
	8		8.7	297.0	--
	9		9.0	388.0	--
	10		10.0	485.0	--
	N_o		6.5	200.0	
	V_s		8.2	281.6	
	α_s		1.44	0.934	

Prestress Ratio s_p	Stress Amplitude S_i ksi	55	34	28	21.4	16
	Specimen No.					
	1	1.4	18.0	49.0	119.2	709.7
	2	1.4	18.0	54.0	125.8	1521.0
	3	1.4	20.0	54.0	191.4	1795.0
	4		20.0	64.0	229.5	2049.6
.75	5		21.0	65.0	237.9	4765.0
	6		21.0	66.0	251.6	5164.0
	7		21.0	68.0	382.3	6700.8
	8		23.0	68.0	456.4	23982.0
	9		25.0	74.0	477.6	--
	10		27.0	79.0	763.0	--
	N_o		15.0	65.0	60.0	280.0
	V_s		22.3	71.4	359.0	58640.0
	α_s		2.22	1.25	1.25	0.832

Prestress Ratio s_p	Stress Amplitude S_i ksi	55	34	10	9.25
	Specimen No.				
	1	1.3	8.5	264.0	606.0
	2	1.3	9.2	312.7	716.0
	3	1.4	9.4	323.4	802.0
	4		9.6	355.4	852.0
-.75	5		9.8	357.5	858.0
	6		9.8	402.1	874.0
	7		10.0	405.5	988.0
	8		10.1	447.0	1114.0
	9		10.7	630.1	1257.0
	10		11.1	1267.9	1763.0
	N_o		8.0	250.0	600.0
	V_s		10.1	476.5	1063.3
	α_s		1.98	0.835	0.70

Prestress Ratio s_p	Stress Amplitude S_i ksi	>5	34	28	25
	Specimen No.				
	1	1.8	40.7	94.0	453.9
	2	1.8	48.0	106.0	--
	3	2.5	49.3	106.0	--
	4		54.5	175.0	--
	5		57.7	188.0	--
1.00	6		58.4	225.0	--
	7		60.7	504.0	--
	8		66.9	2040.0	--
	9		73.2	--	--
	10			--	--
	11			--	
	12			--	
	N_o		35.0	80.0	
	V_s		60.3	216.2	
	α_s		1.85	0.83	

Prestress Ratio s_p	Stress Amplitude S_i ksi	55	34	28	25	22	19	16	13
	Specimen No.								
	1	1.2	12.7	28.2	47.8	78.7	204.1	708.6	3547.1
	2	1.3	13.0	31.3	50.9	94.0	205.0	823.0	4934.4
	3	1.3	13.2	32.8	52.2	95.1	268.0	870.7	7213.0
	4	1.3	13.9	34.2	52.6	103.4	287.0	884.0	14226.4
0	5		14.2	34.5	55.3	110.1	302.0	1193.0	21358.0
	6		15.6	34.9	66.7	125.2	305.0	1637.5	25066.0
	7		16.7	35.2	72.1	129.4	311.0	1796.0	31000.0
	8		17.1	35.4	74.7	163.0	407.0	1996.0	40580.0
	9		19.3	40.9	81.0	166.8	435.0	3653.0	46848.9
	10		21.2	44.6	88.9	179.4	487.0	4660.0	200362.0
	N_o		12.0	25.0	40.0	60.0	150.0	500.0	2000.0
	V_s		16.2	36.8	68.1	134.3	349.0	1847.3	38682.0
	α_s		1.12	2.01	1.56	1.69	1.62	1.00	0.825

Prestress Ratio s_p	Stress Amplitude S_i ksi	55	46	40	37	34
	Specimen No.					
	1	3.3	27.0	99.0	160.0	1043.7
	2	3.7	28.0	101.2	201.0	-1045.9
	3	4.0	29.0	102.9	834.0	24703.0
	4	4.0	33.0	111.8	1113.0	--
	5	4.2	35.0	150.0	1512.0	--
	6	4.7	35.0	150.0	5147.0	--
	7	4.8	35.0	229.7	7096.0	--
1.34	8	4.8	40.0	259.0	8594.0	--
	9	5.2	40.0	279.0	10392.0	--
	10	5.4	41.0	315.0	11318.0	--
	N_o	3.0	25.0	80.0	100.0	
	V_s	4.7	36.0	188.6	4510.0	
	α_s	1.69	1.37	1.01	0.531	

Table 4

Constants of $S - V_s$ Equation (Eq. 5-2), $V_s = A(s - s_e)^{-\nu}$

Prestress Ratio s_p	A	Endurance Limit Ratio s_e	ν
-1.00	364.8	0.0610	2.67
- .75	341.2	0.0610	2.79
0	194.2	0.1341	3.28
.75	171.8	0.1463	3.65
1.00	216.8	0.3049	2.43
1.34	72.3	0.4268	2.96
Smooth	691.0	0.0250	4.76

Table 5

Frequencies of Occurrence p_i of Stress Ratios s_i :

in Exponential Spectra (σ_u = 82,000 psi).

s_i	.35	.45	.55	.65	.75	.85	.95
	.822000	.145600	.026640	.004580	.001000	.00018200	
h=17.3		.822000	.145600	.026640	.004580	.00010000	.00018200
			.822180	.145600	.026640	.00458000	.00100000
	.900000	.090000	.009000	.000900	.000090	.00001000	
h=22.9		.900000	.090000	.009000	.000900	.000090000	.00001000
			.900010	.090000	.009000	.00090000	.00009000
	.968400	.030600	.001000	.000030	.000001	.00000003	
h=34.3		.968400	.030600	.001000	.000030	.00000100	.00000003
			.968400	.030600	.001000	.00003000	.00000100

Table 6

Parameters and Test Results Under (Randomized) Exponential Distributions

Test Series No.	Lowest Stress Level Ratio s_1^*	No. of Stress Levels	h	Prestress Ratio s_p	m	Test Result V'_R (in thousands)	Linear Estimate V_R (in thousands)	Cumulative Cycle Ratio $1/\hat{\omega}$	Endurance Limit Ratio s'_e
23a	.35	6	17.3	0	2.2	609.3	2697.2	0.226	0.068
23b	.35	6	17.3	0	2.25	833.7	3358.2	0.248	0.070
Smooth Specimen	.35	6	17.3	0	1.0	694.3	2099.0	0.331	0.170
24a	.55	5	17.3	0	1.8	52.1	47.0	1.108	0.137
24b	.55	5	17.3	0	2.0	67.5	85.6	0.789	0.110
Smooth Specimen	.55	5	17.3	0	1.0	50.8	118.1	0.430	0.180
25a	.35	6	22.9	0	2.3	2298.0	10062.6	0.228	0.090
Smooth Specimen	.35	6	22.9	0	1.0	1467.4	4413.8	0.332	0.200
26a	.55	5	22.9	0	1.7	41.3	40.1	1.029	0.145
26b	.55	5	22.9	0	1.8	64.8	55.4	1.169	0.137
26c	.55	5	22.9	0	2.0	61.2	102.8	0.595	0.085
Smooth Specimen	.55	5	22.9	0	1.0	52.3	166.6	0.314	0.140
27a	.35	6	34.3	0	2.4	9147.0	60208.3	0.152	0.110
Smooth Specimen	.35	6	34.3	0	1.0	9493.0	7686.4	1.235	0.280
28a	.55	5	34.3	0	2.2	178.0	207.7	0.857	0.125
28b	.55	5	34.3	0	2.3	239.0	292.5	0.817	0.110
Smooth Specimen	.55	5	34.3	0	1.0	92.0	213.0	0.432	0.220

Table 7

Parameters and Test Results Under (Randomized) Exponential Distributions . s^*_i = .45, No. of stress levels = 6

Test Series No.	h	Prestress Ratio s_p	m	Test Result V'_R (in thousands)	Linear Estimate V_R (in thousands)	Cumulative Cycle Ratio $1/\bar{\omega}$	Endurance Limit Ratio s'_e
1a		-1.00	1.4	15.7	10.7	1.467	0.130
1b		-1.00	4.0	222.9	681.1	0.327	0.000
2a		- .75	1.4	18.0	11.8	1.524	0.120
2b		- .75	2.9	206.1	192.1	1.073	0.065
3a		0	1.4	23.5	32.3	0.728	0.100
3b		0	2.3	209.0	739.7	0.283	0.063
4a	17.3	.50	2.1	173.3			
5a		.75	1.4	30.0	57.3	0.524	0.070
5b		.75	1.9	203.7	462.9	0.440	0.090
6a		1.00	1.4	74.9	242.8	0.308	0.230
6b		1.00	1.6	207.4	924.4	0.224	0.220
7a		1.34	1.3	515.4	1574.1	0.328	0.320
7b		1.34	1.4	869.0	4143.7	0.210	0.320
Smooth Specimen		0	1.0	197.5	452.6	0.436	0.220
8a		-1.00	1.4	14.6	11.8	1.237	0.110
8b		-1.00	1.95	85.5	35.1	2.436	0.130
8c		-1.00	4.0	226.3	820.5	0.276	0.000
9a		- .75	1.4	17.9	13.1	1.367	0.120
9b		- .75	3.0	217.0	267.6	0.811	0.057
10a	22.9	0	1.4	24.1	39.5	0.610	0.090
10b		0	1.8	166.4	169.4	0.982	0.132
10c		0	2.0	353.5	360.7	0.979	0.134
10d		0	2.2	370.0	729.0	0.508	0.105
11a		.50	1.8	204.5			
11b		.50	2.1	451.5			
12a		.75	1.4	32.6	73.9	0.442	0.060
12b		.75	1.9	323.4	671.6	0.481	0.110
12c		.75	1.95	468.3	841.3	0.557	0.120
13a		1.00	1.4	89.5	524.4	0.171	0.230
13b	22.9	1.00	1.5	168.2	1250.6	0.134	0.237
14a		1.34	1.3	281.3	8321.5	0.034	0.300
14b		1.34	1.35	1769.3	15173.4	0.117	0.330
14c		1.34	1.4	2715.0	28087.5	0.097	0.310
15a		1.45	1.15	509.0			
Smooth Specimen		0	1.0	220.2	748.5	0.294	0.200
16a		-1.00	1.4	16.9	12.8	1.320	0.110
16b		-1.00	4.0	372.7	945.8	0.394	0.025
17a		- .75	1.4	21.2	14.1	1.501	0.120
17b		- .75	3.5	365.2	597.8	0.611	0.040
18a		0	1.4	27.3	45.9	0.595	0.090
18b		0	2.0	411.6	453.4	0.908	0.128
18c	34.3	0	2.3	559.0	1502.5	0.372	0.025
19a		.50	2.1	518.5			
20a		.75	1.4	39.4	79.3	0.497	0.070
20b		.75	1.8	347.9	569.7	0.611	0.122
21a		1.00	1.4	97.7	1478.8	0.066	0.230
21b		1.00	1.5	377.4	5409.8	0.070	0.250
22a		1.34	1.25	517.4	26683.0	0.019	0.300
22b		1.34	1.4	5200.0	652000.0	0.009	0.300
Smooth Specimen		0	1.0	336.1	1063.6	0.316	0.210

Table 8

Number of Cycles to Failure, N_R', in Thousands, Under (Randomized) Exponential Distributions (see Tables 6 and 7)

Specimen Number	Test Series No. 1a	1b	2a	2b	3a	3b	4a	5a	5b	6a
1	13.1	172.7	16.8	152.1	18.1	172.1	123.6	24.4	128.9	59.2
2	13.5	187.6	16.8	180.9	20.9	179.8	127.0	25.9	129.3	59.4
3	13.8	193.5	16.9	181.8	21.2	190.5	134.8	26.8	132.1	60.0
4	14.1	194.7	17.1	185.5	21.6	192.3	136.8	27.3	176.4	62.6
5	15.1	198.7	17.2	196.6	22.0	203.3	148.2	27.4	189.0	68.0
6	15.1	210.7	17.9	198.0	22.1	204.3	171.7	29.1	199.0	69.8
7	15.2	213.0	18.0	200.3	22.7	205.8	171.9	30.0	209.9	77.5
8	15.8	224.6	18.4	202.4	24.6	214.3	188.9	31.2	228.1	83.6
9	18.1	260.4	18.9	208.8	24.6	222.0	211.1	31.6	242.5	88.9
10	19.4	272.9	19.7	255.4	27.2	228.5	221.7	36.0	245.5	97.4
N_o	12.5	140.0	16.0	130.0	15.0	150.0	100.0	22.0	100.0	55.0
V_R'	15.7	222.9	18.0	206.1	23.5	209.0	173.3	30.0	203.7	74.9
a_R	1.38	2.36	1.79	2.27	2.72	2.49	1.71	1.98	1.52	1.14

Specimen Number	Test Series No. 14b	14c	15a	16a	16b	17a	17b	18a	18b	18c
1	422.2	609.3	89.4	14.4	319.5	18.4	259.5	23.7	209.0	288.8
2	581.6	1112.1	161.2	14.9	329.9	18.4	304.2	24.0	297.6	350.0
3	657.6	1136.2	251.4	16.1	335.0	19.9	322.2	24.6	330.2	364.3
4	787.7	1212.2	253.9	16.1	361.5	20.0	336.7	25.0	346.9	370.0
5	858.4	1536.7	331.2	16.3	364.6	20.1	344.2	25.7	371.7	372.8
6	1487.5	2008.5	378.0	17.0	365.5	21.0	350.8	26.5	392.7	457.8
7	1939.2	2279.3	446.1	17.1	377.7	21.0	368.2	26.7	394.7	489.8
8	2351.4	3360.7	565.0	17.3	380.5	21.5	369.4	27.5	452.3	685.8
9	3441.5	5556.6	673.0	17.7	391.3	22.5	379.1	30.0	467.3	832.4
10	3570.5	6463.6	1379.1	17.9	397.0	23.1	432.7	33.0	472.0	879.3
N_o	200.0	400.0	5.0	13.0	300.0	15.0	150.0	22.0	80.0	150.0
V_R'	1769.5	2715.0	509.0	16.9	372.7	21.2	365.2	27.3	411.6	559.0
a_R	1.06	0.983	1.28	2.64	1.88	3.41	4.28	1.75	3.00	1.78

Specimen Number	Test Series No. 6b	7a	7b	8a	8b	8c	9a	9b	10a	10b
1	106.8	134.4	545.4	11.6	52.0	194.3	15.0	175.6	22.0	134.3
2	135.5	140.6	594.0	12.6	53.7	194.5	15.7	192.3	22.2	140.4
3	138.9	208.4	670.4	13.4	57.1	200.0	16.2	196.0	22.2	152.2
4	163.5	314.9	675.5	14.2	75.2	212.1	17.3	199.4	22.8	152.5
5	177.6	442.5	763.2	14.3	79.4	219.2	17.4	200.9	22.9	156.9
6	184.5	567.9	807.7	14.4	81.1	222.2	17.5	204.1	23.5	164.5
7	194.0	618.5	809.7	14.7	90.2	228.7	18.2	216.3	24.4	166.5
8	200.7	686.7	1007.9	15.0	96.0	234.4	18.4	226.5	24.7	174.5
9	251.8	707.0	1012.8	15.1	99.9	239.8	18.6	236.0	24.9	177.9
10	340.0	768.5	1310.2	16.0	104.1	242.6	18.8	245.8	27.8	181.7
N_o	70.0	100.0	500.0	10.0	40.0	180.0	14.0	160.0	21.0	120.0
V_R'	207.4	515.4	869.0	14.6	85.5	226.3	17.9	217.0	24.1	166.4
a_R	1.80	0.866	1.17	2.94	1.58	1.63	1.97	1.80	1.61	2.13

Specimen Number	Test Series No. 19a	20a	20b	21a	21b	22a	22b	23a	23b	24a
1	152.8	29.3	144.4	48.2	131.5	123.8	1024.4	431.1	463.4	40.7
2	212.4	33.6	189.3	54.6	169.4	139.6	1181.4	452.7	590.5	40.8
3	277.9	33.6	208.0	55.7	205.0	148.5	1360.6	456.1	631.9	41.2
4	308.9	34.2	218.1	67.5	222.1	168.9	1880.0	481.1	653.2	43.5
5	336.6	36.9	231.5	70.0	245.0	177.3	2208.8	540.7	686.2	44.5
6	466.6	39.3	239.0	79.3	304.4	639.5	2544.8	563.7	761.7	46.9
7	496.7	40.1	242.3	102.9	486.6	698.6	4457.6	583.4	876.9	52.4
8	693.7	40.8	381.7	120.2	543.9	939.0	8511.8	615.2	932.3	58.5
9	698.7	41.0	595.8	121.4	571.3	1056.5	---	654.6	982.0	60.2
10	927.2	46.1	803.8	206.0	597.1	1370.6	---	695.0	1045.5	71.6
11								864.2		
N_o	60.0	27.0	120.0	40.0	70.0	100.0	900.0	350.0	350.0	35.0
V_R'	518.5	39.4	347.9	97.7	377.4	517.4	6000.0	609.3	833.7	52.1
a_R	1.42	1.63	1.04	1.08	1.33	0.650	0.586	1.77	1.82	1.49
L_o	0.00	0.00	0.00	0.00	0.00	0.00	0.1818	0.00	0.00	0.00

Specimen Number	Test Series No. 10c	10d	11a	11b	12a	12b	12c	13a	13b	14a
1	257.3	187.4	110.7	217.8	25.3	181.0	357.0	69.3	102.6	99.3
2	271.0	230.6	157.9	368.6	26.8	187.5	384.2	73.9	118.9	102.2
3	285.6	265.4	169.4	392.4	26.9	250.6	397.8	77.2	124.2	133.5
4	299.6	311.6	182.5	396.3	27.5	255.0	420.7	80.6	126.9	155.2
5	301.9	329.8	189.9	417.1	32.4	284.7	425.9	85.1	143.9	159.3
6	333.7	348.6	194.2	442.2	32.8	323.9	447.8	89.2	148.6	270.5
7	364.5	375.1	194.7	446.9	33.0	345.8	469.6	89.4	180.7	318.8
8	373.3	407.0	219.4	452.2	35.3	353.4	478.6	94.6	183.1	372.4
9	412.7	427.4	224.5	461.1	35.8	367.2	515.3	96.7	193.4	421.6
10	467.1	465.1	228.6	499.4	37.8	387.7	570.0	99.5	263.0	493.3
N_o	230.0	120.0	60.0	100.0	24.0	100.0	300.0	60.0	95.0	50.0
V_R'	353.0	370.0	204.5	451.5	32.6	323.4	468.3	89.6	168.2	281.3
a_R	1.46	1.97	2.84	2.91	1.26	2.21	2.17	2.14	1.13	1.23

Specimen Number	Test Series No. 24b	25a	26a	26b	26c	27a	28a	28b
1	45.2	1168.9	32.4	39.4	34.2	3931.9	107.1	127.3
2	47.8	1178.7	35.0	53.5	46.8	4038.3	120.6	145.1
3	49.8	1185.7	36.2	56.8	49.3	5240.2	135.0	185.1
4	63.3	1478.0	37.1	59.4	51.4	6105.2	138.1	192.3
5	65.8	1479.0	37.2	60.0	52.8	6146.6	157.3	193.8
6	67.5	1584.9	40.5	62.7	54.5	6820.6	163.2	198.2
7	68.5	1693.0	41.7	63.8	63.1	7429.7	179.3	239.4
8	72.0	1990.3	42.2	65.0	64.2	8516.5	191.1	303.2
9	74.5	2022.2	42.6	67.7	65.1	10422.6	211.7	310.2
10	76.9	2583.0	52.4	69.4	78.8	11624.3	246.3	310.5
11		2851.4				12570.8		
12		3088.7				16640.0		
13		3770.2						
14		4928.1						
N_o	40.0	1000.0	30.0	35.0	30.0	2000.0	90.0	100.0
V_R'	67.5	2298.0	41.3	64.8	61.2	9147.0	178.0	239.0
a_R	1.43	1.02	1.63	1.66	1.49	1.64	1.50	1.49

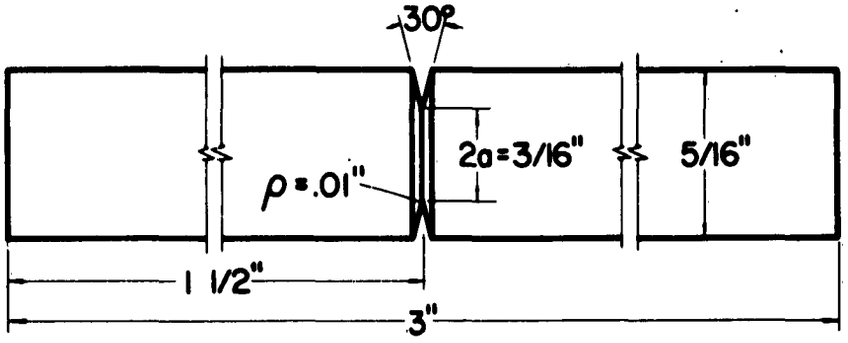

Fig. 1 Notch Geometry.

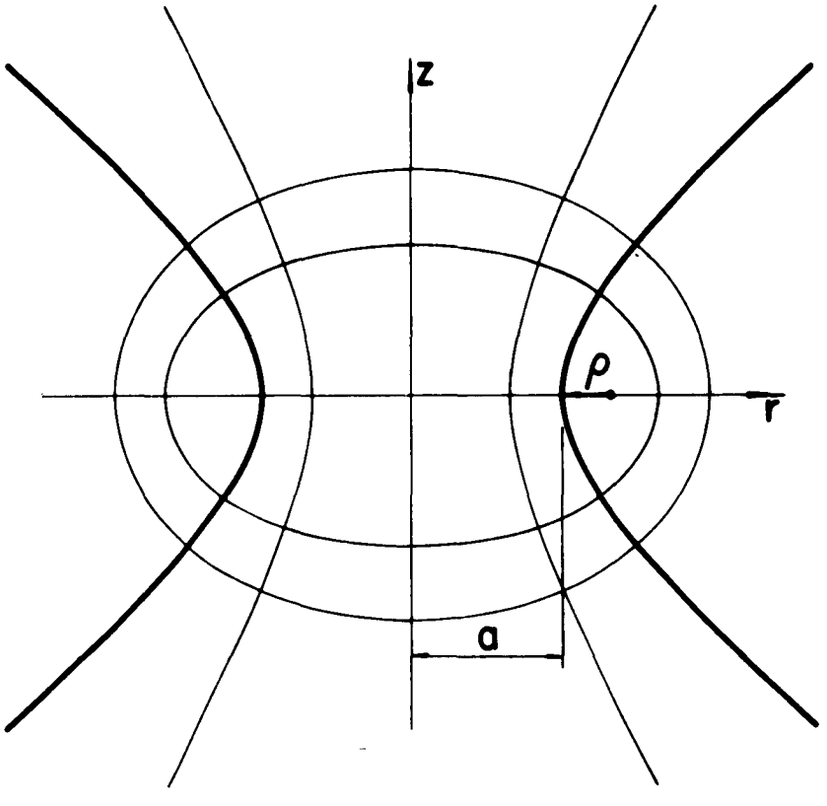

Fig. 2 Oblate Spheroidal Coordinate System for Circumferential Hyperbolic Notch.

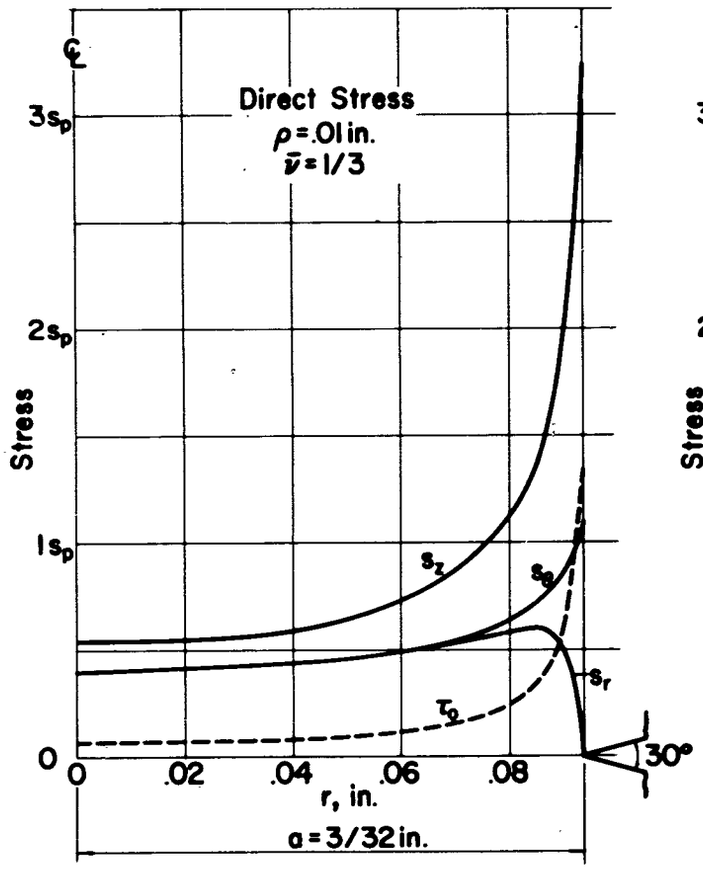

Fig. 3 Elastic Stress Distribution at the Minimum Cross Section for Direct Longitudinal Load

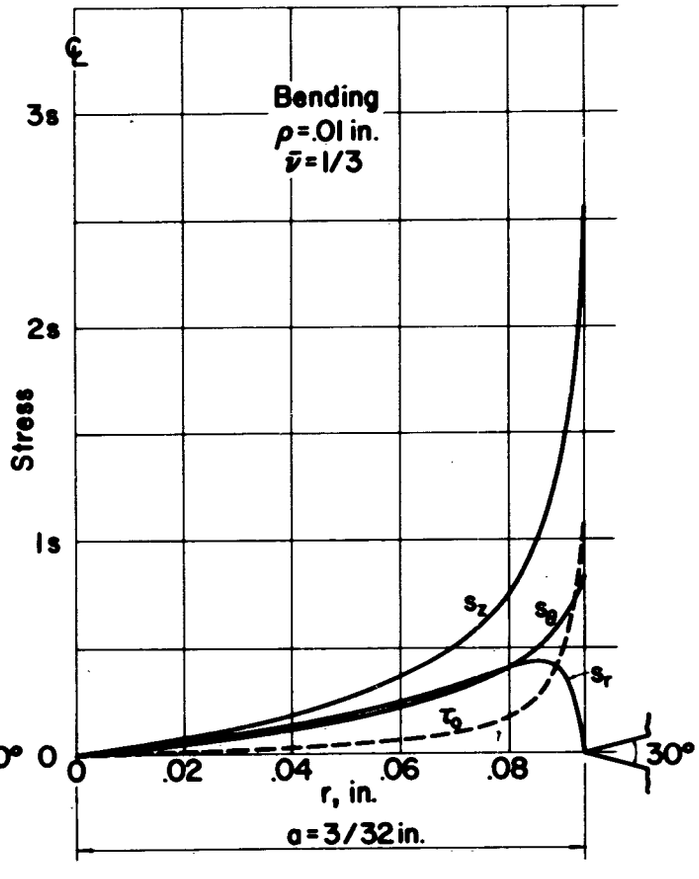

Fig. 4 Elastic Stress Distribution at the Minimum Cross Section for Bending

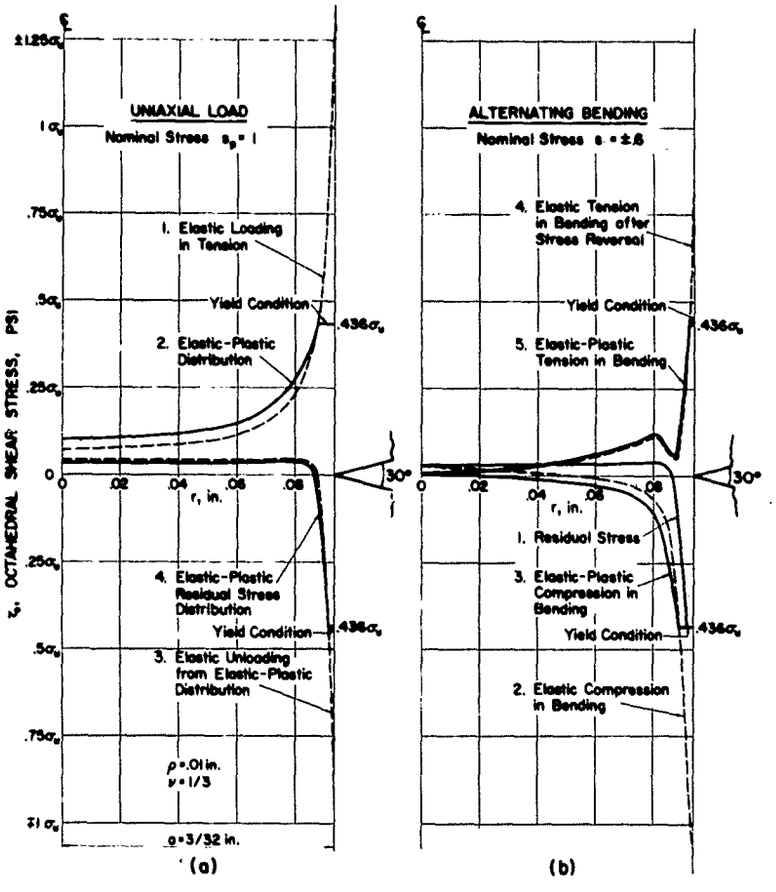

Fig. 5 Development of Residual Stress Field due to Direct Stress $s_p = 1$(a) and Superimposed Alternating Bending Stress $s = .6$(b)

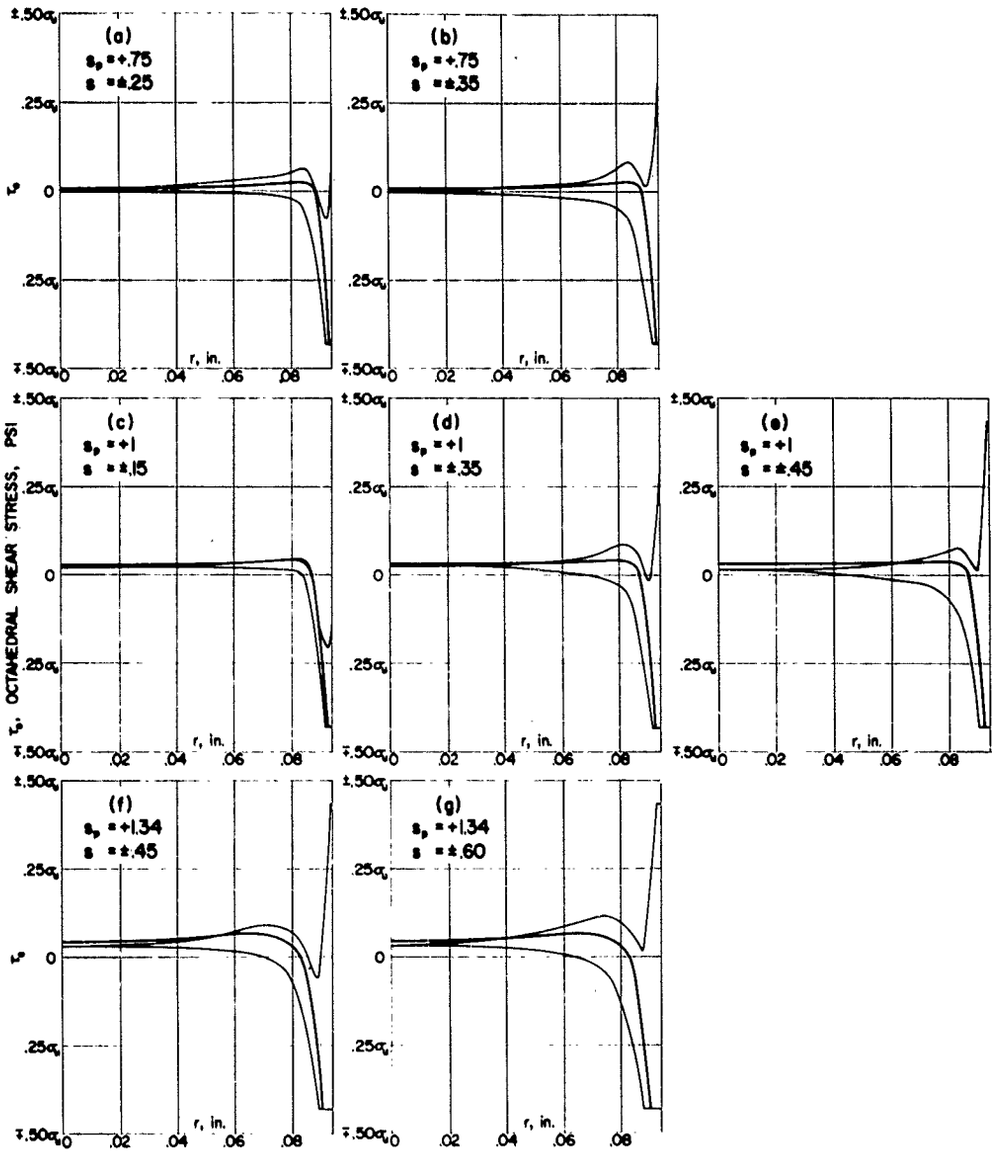

Fig. 6 Alternating Bending Stress Superimposed on Residual Stress for Various Values of s_p and s

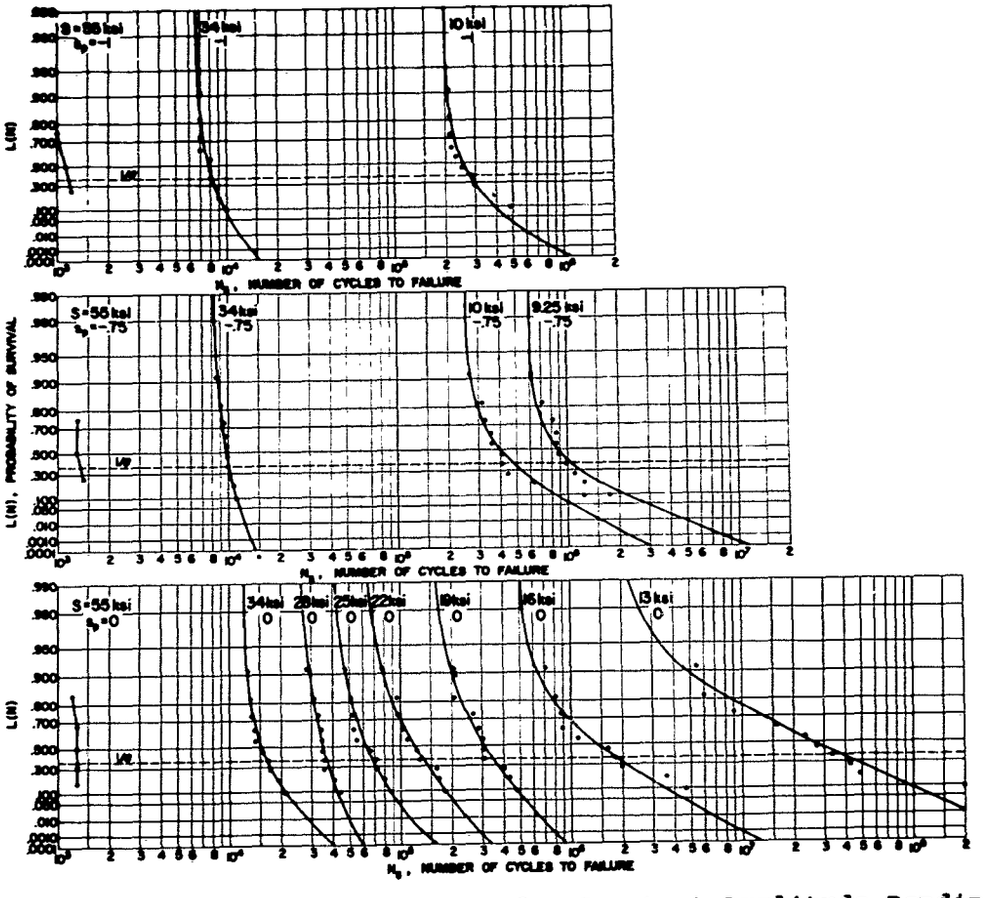

Fig. 7a Survivorship Functions for Constant Amplitude Bending Stress and Direct Prestress.

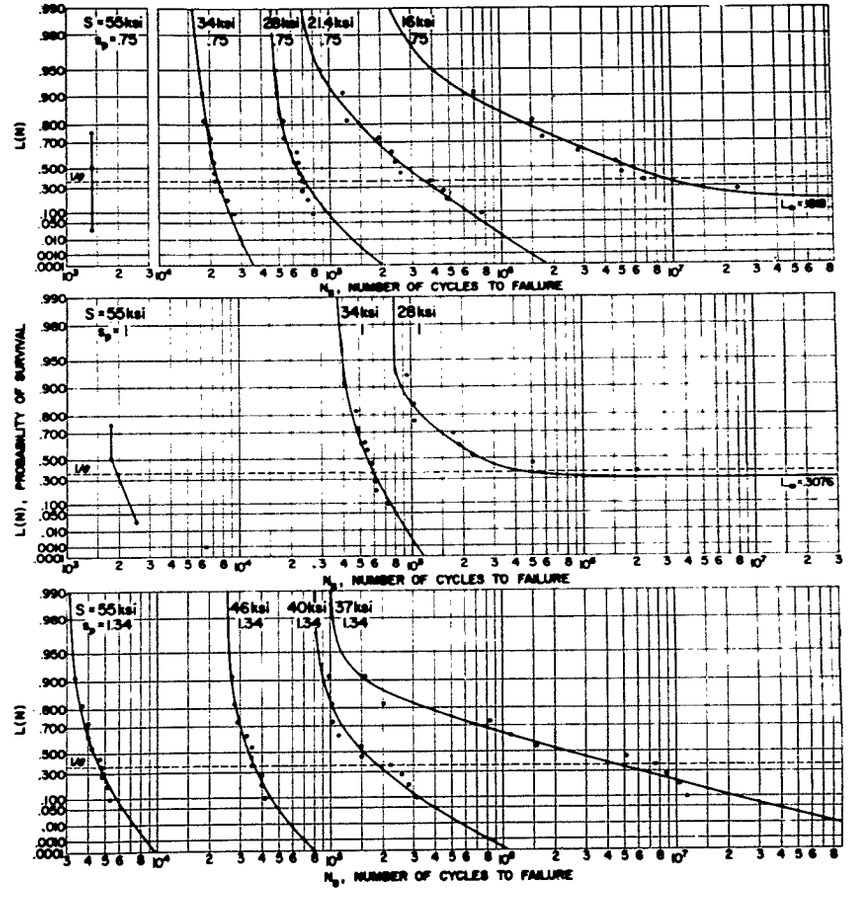

Fig. 7b Survivorship Functions for Constant Amplitude Bending Stress and Direct Prestress.

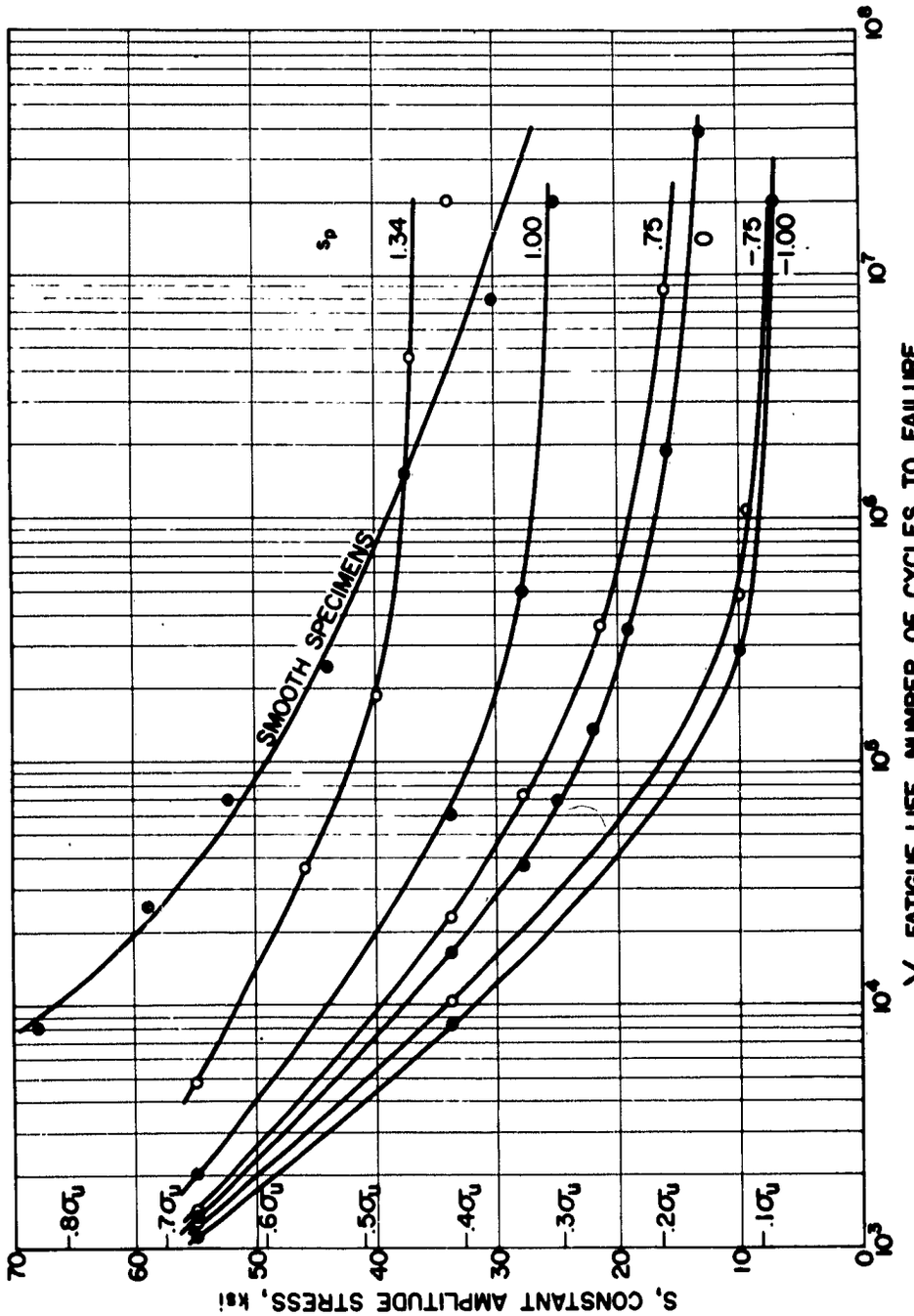

Fig. 8 Constant Amplitude S - N_f Diagrams for Smooth and Notched Specimens with Various Amounts of Prestress

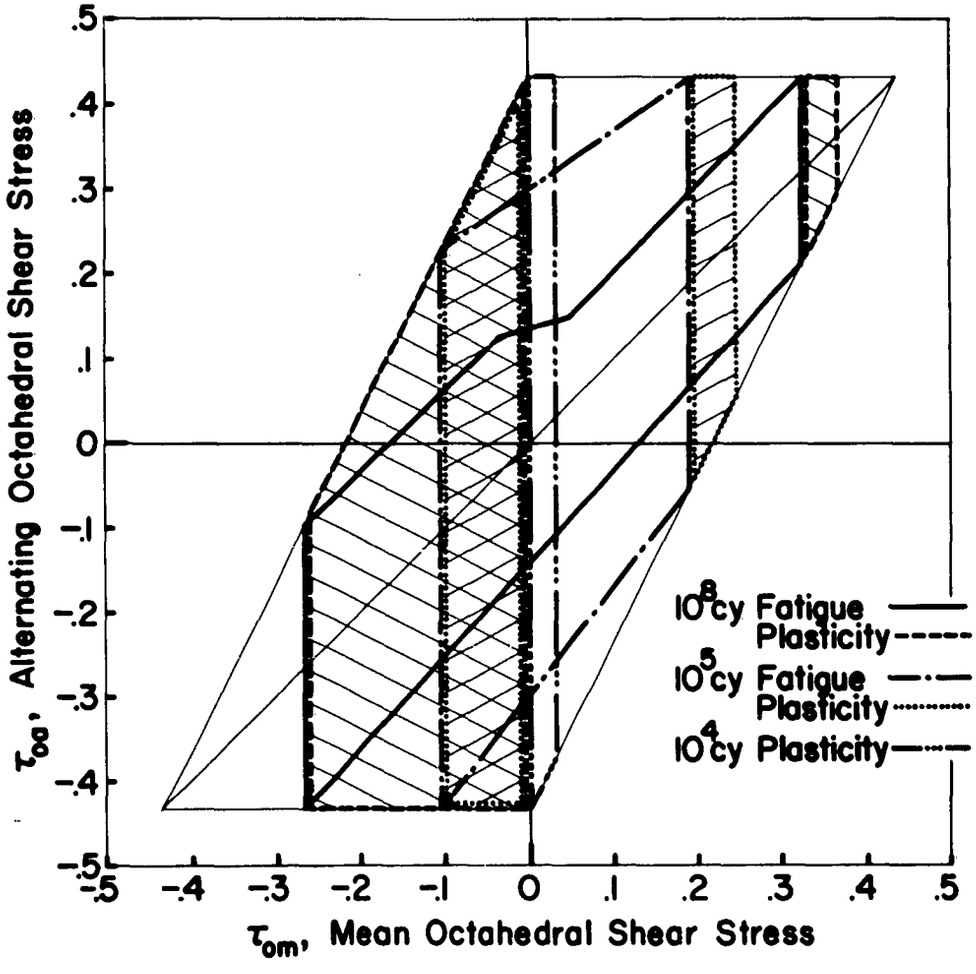

Fig. 9 Modified Goodman Diagrams

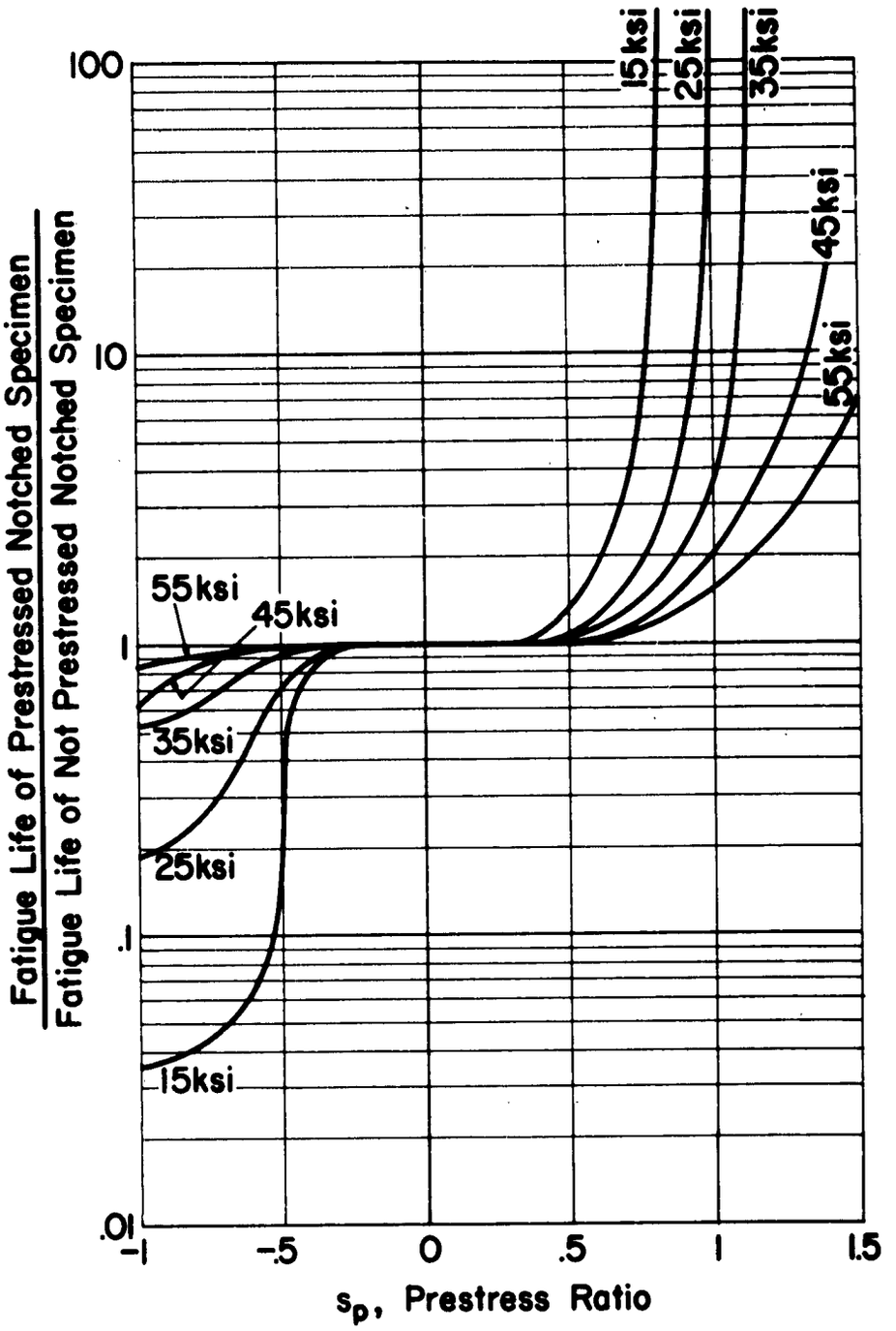

Fig. 10 Ratio of Constant Amplitude Fatigue Lives of Pre-Stressed and Non-Prestressed Notched Specimens as a Function of Prestress

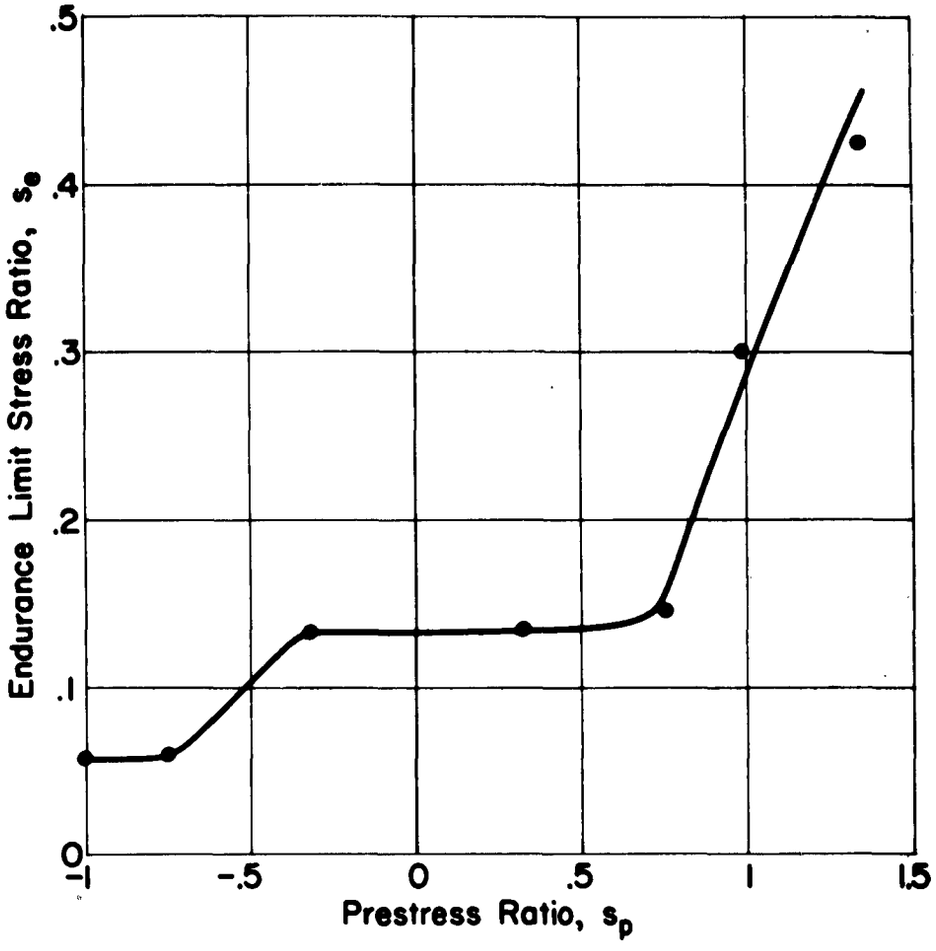

Fig. 11 Conventional Constant Amplitude Endurance Limit as a Function of Prestress

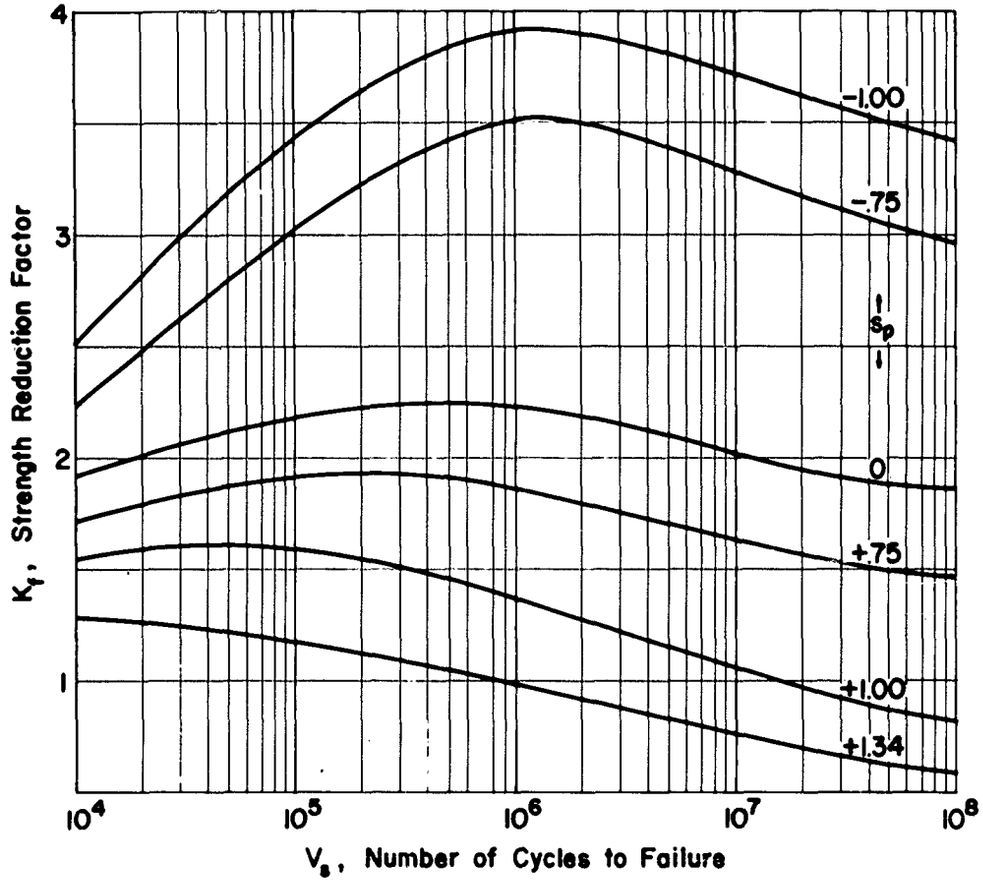

Fig. 12 Constant Amplitude Strength Reduction Factor as a Function of Fatigue Life

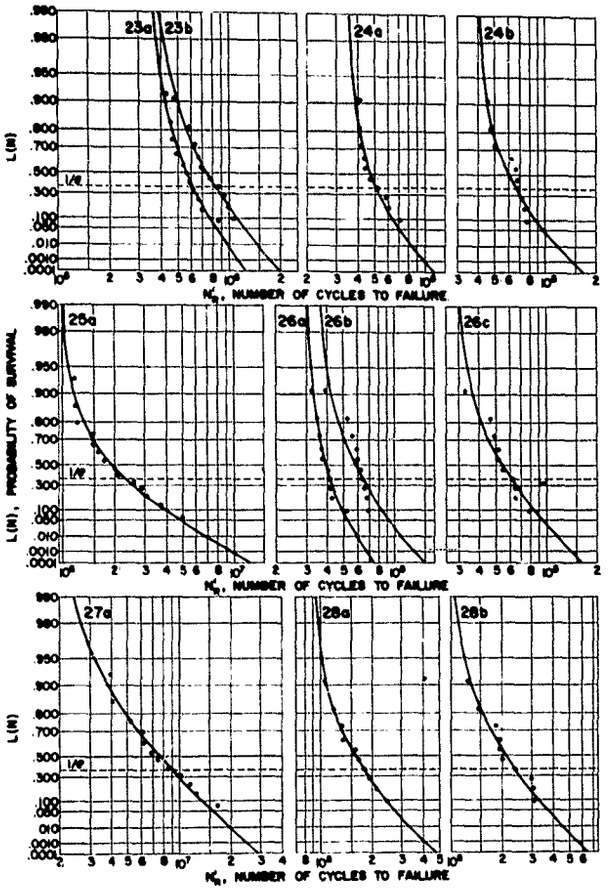

Fig. 13a Survivorship Functions for Notched Specimens Under (Randomized) Exponential Stress Distributions (see Tables 6 and 8); $s_p = 0$

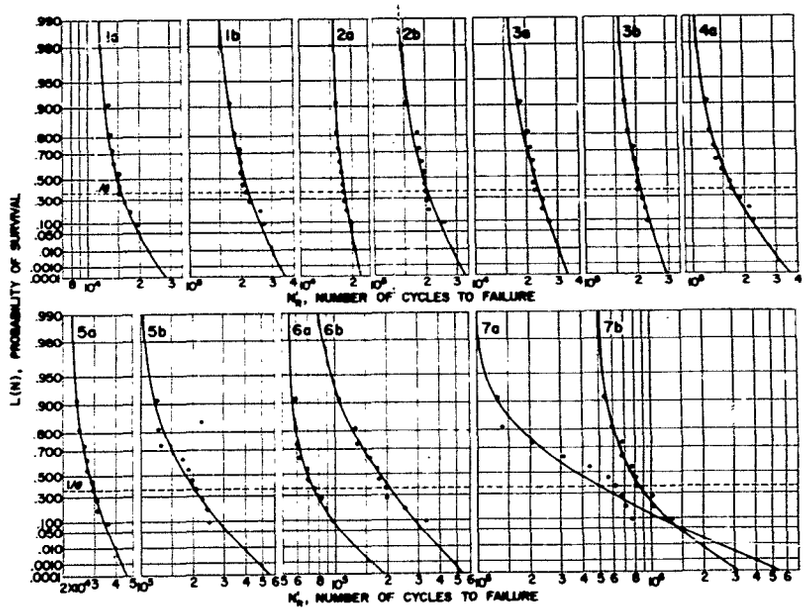

Fig. 13b Survivorship Functions for Notched Specimens Under (Randomized) Exponential Stress Distributions with Prestress; h = 17.3, $s_1^* = .45$ (see Tables 7 and 8).

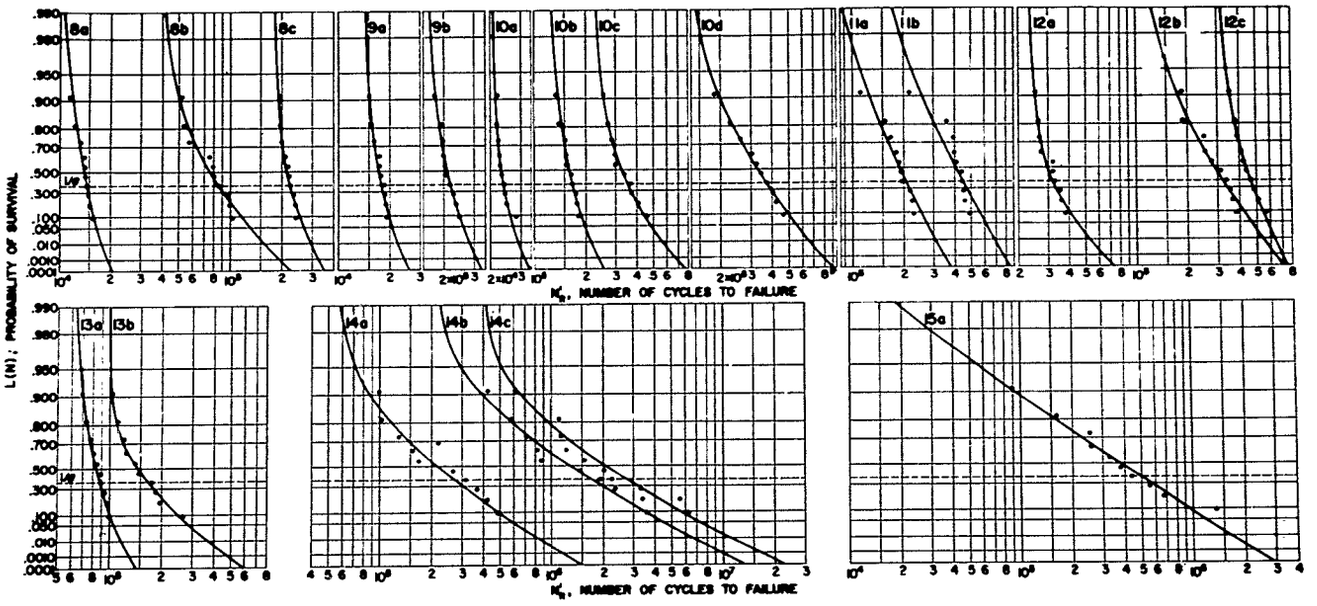

Fig. 13c Survivorship Functions for Notched Specimens Under (Randomized) Exponential Stress Distributions with Prestress; h = 22.9, $s_1^* = .45$ (see Tables 7 and 8).

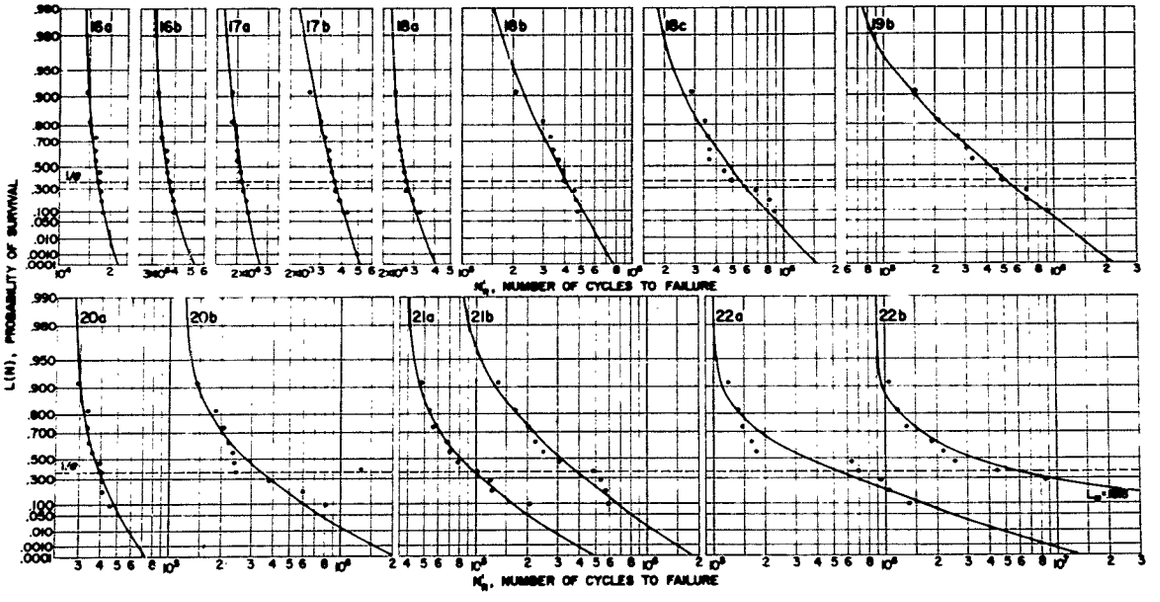

Fig. 13d Survivorship Functions for Notched Specimens Under (Randomized) Exponential Stress Distributions with Prestress; $h = 34.3$, $s_1^* = .45$ (see Tables 7 and 8).

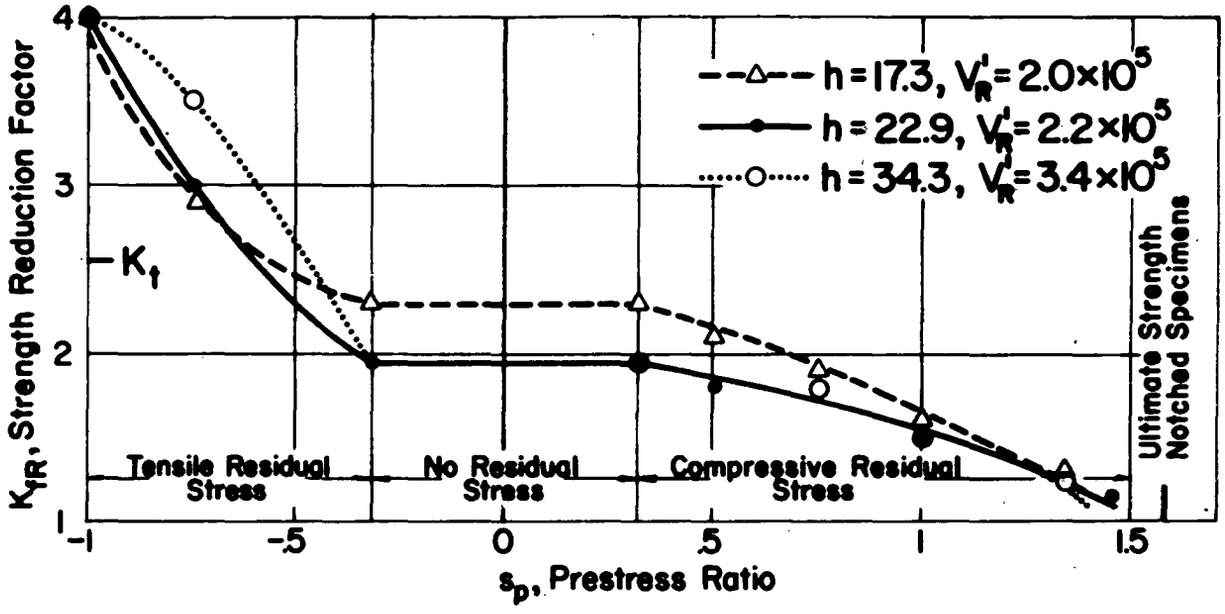

Fig. 14 Random Strength Reduction Factor as a Function of Prestress; s_1 = .45/m , Δs = .1/m, No. of stress levels = 6

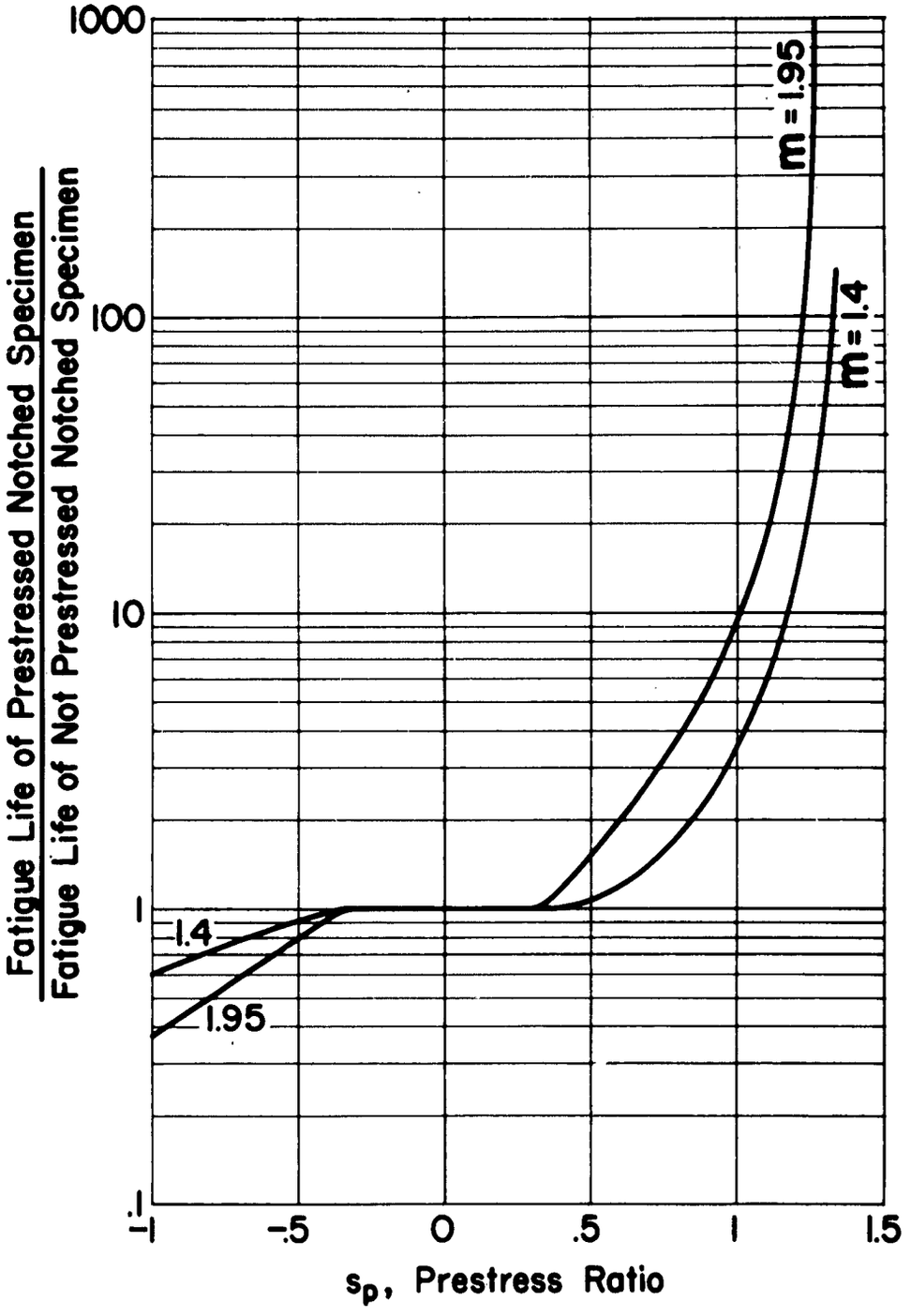

Fig. 15 Ratio of Random Fatigue Lives of Prestressed and Non-Prestressed Notched Specimens as a Function of Prestress for Two Values of m ; $s_1 = .45/m$, $\Delta s = .1/m$, No. of stress levels = 6

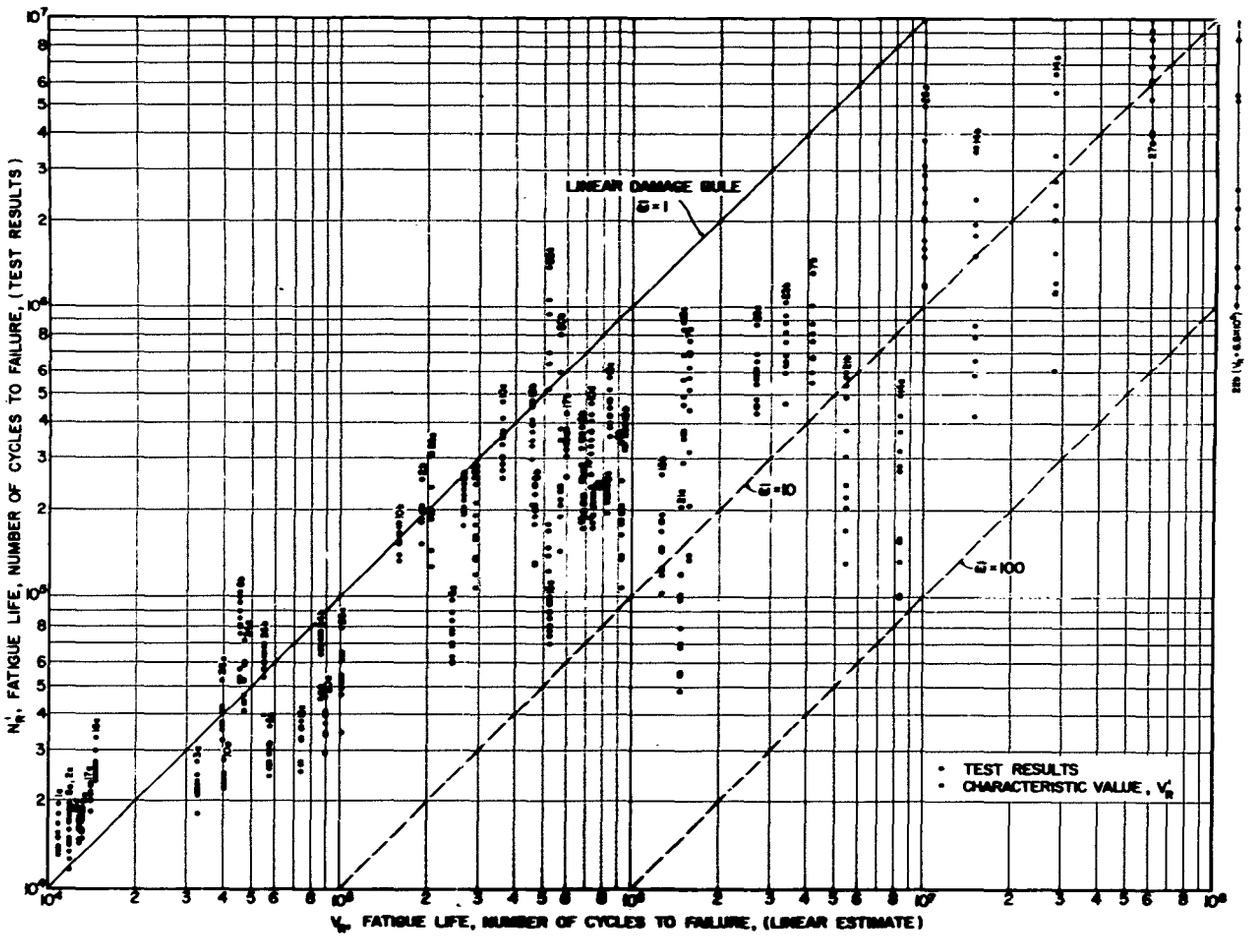

Fig. 16 Deviation of Random Fatigue Test Results N'_R from Linear Estimate V_R

Aeronautical Systems Division, Dir/Materials and Processes, Metals and Ceramics Lab. Wright-Patterson AFB, Ohio.
Rpt No. ASD-TDR-62-1075 INFLUENCE OF RESIDUAL STRESSES ON RANDOM FATIGUE LIFE, IN BENDING, OF NOTCHED 7075 ALUMINUM SPECIMENS. Summary report, Dec 62, 52pp. incl illus, tables, 20 refs.

Unclassified report

Theoretical and experimental results of investigations conducted to determine the effects of residual stresses on fatigue damage accumulation and fatigue life under both constant amplitude and randomized exponential stress distributions, of 7075-T6 circumferentially notched rotating bending

(over)

1. Aluminum Fatigue
2. Strain-Aging Effects on Aluminum
3. Plasticity of Al
I. AFSC Project 7351, Task 735106
II. Contract AF 33 (616)-7042
III. Columbia University New York, N. Y.
IV. R. A. Heller, M. Seki, A. M. Freudenthal
V. Aval fr OTS
VI. In ASTIA collection

Aeronautical Systems Division, Dir/Materials and Processes, Metals and Ceramics Lab. Wright-Patterson AFB, Ohio.
Rpt No. ASD-TDR-62-1075 INFLUENCE OF RESIDUAL STRESSES ON RANDOM FATIGUE LIFE, IN BENDING, OF NOTCHED 7075 ALUMINUM SPECIMENS. Summary report, Dec 62, 52pp. incl illus, tables, 20 refs.

Unclassified report

Theoretical and experimental results of investigations conducted to determine the effects of residual stresses on fatigue damage accumulation and fatigue life under both constant amplitude and randomized exponential stress distributions, of 7075-T6 circumferentially notched rotating bending

(over)

1. Aluminum Fatigue
2. Strain-Aging Effects on Aluminum
3. Plasticity of Al
I. AFSC Project 7351, Task 735106
II. Contract AF 33 (616)-7042
III. Columbia University New York, N. Y.
IV. R. A. Heller, M. Seki, A. M. Freudenthal
V. Aval fr OTS
VI. In ASTIA collection

specimens are presented. The variation of the strength reduction factor as a function of prestress and load spectrum is examined. An approximate analysis of the elastic-plastic stress distribution at the minimum cross-section is suggested on the basis of which fatigue behavior can be predicted. The results indicate that the linear (Miner) cumulative damage rule quite generally overestimates fatigue lives except in the alternating plasticity range and that the endurance limit is considerably reduced as a result of stress interaction, provided that in the application of the linear damage rule the S-N diagram for the prestressed specimen is used. In the range of alternating plasticity at the root of the notch $10^3 < N < 10^4$ the linear rule consistently underestimates the fatigue life.

specimens are presented. The variation of the strength reduction factor as a function of prestress and load spectrum is examined. An approximate analysis of the elastic-plastic stress distribution at the minimum cross-section is suggested on the basis of which fatigue behavior can be predicted. The results indicate that the linear (Miner) cumulative damage rule quite generally overestimates fatigue lives except in the alternating plasticity range and that the endurance limit is considerably reduced as a result of stress interaction, provided that in the application of the linear damage rule the S-N diagram for the prestressed specimen is used. In the range of alternating plasticity at the root of the notch $10^3 < N < 10^4$ the linear rule consistently underestimates the fatigue life.